



Metallurgy Department. Progress Report for the Period 1 January to 31 December 1984

Risø National Laboratory, Roskilde

Publication date:
1985

Document Version
Publisher's PDF, also known as Version of record

[Link back to DTU Orbit](#)

Citation (APA):
Risø National Laboratory, R. (1985). *Metallurgy Department. Progress Report for the Period 1 January to 31 December 1984*. Risø National Laboratory. Denmark. Forskningscenter Risoe. Risoe-R No. 523

General rights

Copyright and moral rights for the publications made accessible in the public portal are retained by the authors and/or other copyright owners and it is a condition of accessing publications that users recognise and abide by the legal requirements associated with these rights.

- Users may download and print one copy of any publication from the public portal for the purpose of private study or research.
- You may not further distribute the material or use it for any profit-making activity or commercial gain
- You may freely distribute the URL identifying the publication in the public portal

If you believe that this document breaches copyright please contact us providing details, and we will remove access to the work immediately and investigate your claim.

Metallurgy Department Progress Report for the Period 1 January to 31 December 1984

Risø-R-523

METALLURGY DEPARTMENT PROGRESS REPORT FOR THE PERIOD
1 JANUARY TO 31 DECEMBER 1984

Abstract. The activities of the Metallurgy Department at Risø during 1984 are described. The work is presented in three chapters: General Materials Research, Technology and Materials Development, and Fuel Elements. A survey is given of the Department's participation in international collaboration and of its activities within education and training. A list (with abstracts) of publications and lectures by the staff during 1984 is included.

INIS-descriptors: FUEL ELEMENTS, METALLURGY, NONDESTRUCTIVE TESTING, RESEARCH PROGRAMS, RISØE NATIONAL LABORATORY.

UDC 669

April 1985

Risø National Laboratory, DK-4000 Roskilde, Denmark

ISBN 87-550-1103-9
ISSN 0106-2840

Risø Repro 1985

CONTENTS

	Page
1. INTRODUCTION	5
2. GENERAL MATERIALS RESEARCH	7
2.1. Recrystallization and grain growth in particle containing materials	7
2.2. Neutron diffraction facility for in-situ texture measurements	8
2.3. Texture development during recrystallization of commercially pure aluminium	9
2.4. Calorimetric studies of recrystallization	9
2.5. Small angle neutron scattering study of γ' -precipitation	10
2.6. Creep in fcc metals	11
2.7. Plastic deformation of composites	12
2.8. Fatigue in metals	13
2.9. Plastic deformation of polycrystals	15
2.10. Irradiation of high-purity aluminium with 600 and 800 MeV protons	18
2.11. Accumulation of gas atoms at grain boundaries during irradiation	19
2.12. Nucleation and growth of microstructural inhomogeneity during irradiation	20
2.13. Quasielastic neutron scattering studies of the ionic conductors $Ba_{1-x}U_xF_{2+2x}$	22
2.14. Oxygen conductors and electrode materials for fuel cells	23
3. TECHNOLOGY AND MATERIALS DEVELOPMENT	24
3.1. Fatigue testing	24
3.2. Fracture testing	25
3.3. Brazing and soldering	26
3.4. High temperature corrosion	26
3.5. Fibre reinforced plastics	27
3.6. Damage in laminates	28

	Page
3.7. Metal-hydrogen systems	28
3.8. Lithium electrodes for non-reversible batteries	30
3.9. Solid electrolyte research	30
3.10. Oxygen conductors	31
3.11. High temperature oxygen-gas sensors	33
3.12. Non-destructive testing	34
4. FUEL ELEMENTS	36
4.1. UO ₂ -Zr irradiations	36
4.2. The Risø Transient Fission Gas Release Project	37
4.3. Continuous, on-line monitoring of internal fuel pin pressure	37
4.4. Local gas release and swelling in UO ₂ fuel during slow transient	38
5. PARTICIPATION IN INTERNATIONAL COLLABORATION	40
6. EDUCATION AND TRAINING	42
PUBLICATIONS	- 43 -
LECTURES	- 58 -
STAFF OF THE DEPARTMENT	- 74 -

1. INTRODUCTION

The activities of the Metallurgy Department over the last 5-10 years have gradually changed from being concentrated mainly on nuclear metallurgy to covering a number of different areas within materials science and engineering. This work is presented in three chapters: General Materials Research, Technology and Material Developments and Fuel Elements. Under these headings projects are described which extend from fundamental materials research to industrial projects on materials application. Most of the projects relate to energy applications as in fuel element research, development of light and strong materials and characterization of materials to be used in energy storage systems. Projects of a more general nature are carried out within the areas of fatigue and creep, non-destructive testing, neutronradiography and ceramics. The joint work with the Physics Department is continued on neutron diffraction for in-situ texture measurements and on small angle neutron scattering for studying processes such as precipitation and radiation damage. The many new research areas have required procurement of new equipment, e.g. a scanning microscope, a pulsator for fatigue testing and apparatus for sputtering. Furthermore the automation of existing equipment have been continued. Most of the purchases to the department has been financed through income from contract research, which is now covering about 30 per cent of the total activities.

The department participated in international collaboration on specific research projects and study groups under the auspices of EEC, NEA, IAEA and various nordic and US organizations. The department organized the 5th Risø International Symposium on Metallurgy and Materials Science, 3-7 September 1984. The title of this symposium was "Microstructural Characterization of Materials by Non-Microscopical Techniques". The Symposium was attended by approximately 100 participants and 75 papers were presented. Planning was started for the 6th International Symposium

to be held at Risø 9-13 September 1985. The title of the symposium is: "Transport-Structure Relations in Fast Ion and Mixed Conductors". Educational activities were continued, students and graduates from Denmark and abroad studied in the Department.

2. GENERAL MATERIALS RESEARCH

The materials research programme includes long-term experimental and theoretical studies aimed at contributing to an understanding of the physical mechanisms governing the properties of materials of general technological interest. A large part of this work is carried out in collaboration with universities and research laboratories in Denmark and abroad. Major efforts are devoted to materials preparation and testing and to microstructural characterization by a variety of microscopical and non-microscopical techniques. The relation between the observed macroscopic and microscopic behaviour is studied theoretically in terms of crystal lattice defects by computer methods and combinations of continuum models and discrete models. The research topics include recrystallisation, grain growth and texture evolution (2.1-2.4), precipitation of particles (2.5), high temperature deformation (2.6), low temperature deformation and fatigue (2.7-2.9), irradiation damage (2.10-2.12), and solid state ion transport (2.13-2.14). The materials under investigation cover metals and alloys, composite materials and ceramics. The research results are published in the open literature.

2.1. Recrystallization and grain growth in particle containing materials

(In collaboration with the Danish Academy of Engineering)

The work on grain growth after recrystallization in aluminium with a fine dispersion of fine alumina particles was concluded. A new programme was initiated with the aim of studying the effect of small particles on the texture development during recrystallization and grain growth. In-situ texture measurements were carried out using neutron diffraction techniques and information was obtained both about the composition of the recrystallization texture and the kinetics of formation of the individual texture components. In parallel with the texture measurements

a simultaneous determination of both the orientation and size of individual recrystallized grains was obtained by selected area channelling patterns.

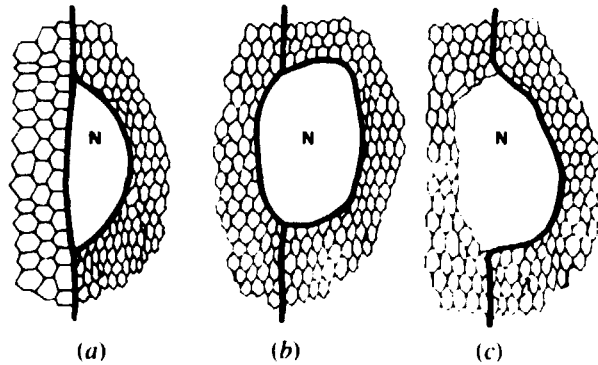


Fig. 1. Schematic drawing showing 3 types of grain boundary nuclei marked by N. The hexagonal networks are the subgrains. In (a) the nucleus is formed by subgrain growth to the right of the original grain boundary. In (b) the nucleus is formed by grain boundary migration to the right and subgrain growth to the left forming a new high-angle boundary. In (c) the nucleus is formed by grain boundary migration to the right, whereas subgrain growth has taken place to the left without forming a new high-angle boundary.

2.2. Neutron diffraction facility for in-situ texture measurements

Improvements were made of the neutron diffraction facility for in-situ texture measurements. The basic unit was changed from being the standard triple-axis spectrometer TAS 7 to the newly developed multipurpose spectrometer TAS 3 at DR 3. TAS 3 is designed to work with one of three different detector systems and the change between the systems is very easy. For the texture measurements this means that the start up time for each measuring period is reduced from more than half a day to about one hour. Furthermore, a CANON-AS 100 computer with a colour screen and an 8 colour jet-ink plotter was installed to provide on-line graphical representation of the measured data.

2.3. Texture development during recrystallization of commercially pure aluminium

(In collaboration with the Department of Metallurgy and Materials Science, Imperial College, London)

The recrystallization process in heavily deformed (90% cold rolled) commercially pure (99.5%) aluminium containing large intermetallic particles was studied by in-situ neutron diffraction texture measurements and various microscopical technique including texture measurements in local areas and simultaneous determination of size and orientation of individual grains. The formation and growth of recrystallization nuclei at the particles and in the matrix were examined by correlating the measured change in texture with the observed change in microstructure. The orientation of the nuclei and their rate of formation and growth determines the recrystallization texture, which is found to consists of cube, rolling and random components. The randomly oriented grains nucleated at particles show a fast nucleation rate and a low growth rate, whereas the grains of cube orientation, characteristic of pure aluminium, are relatively few but have the highest growth rate. As a result the presence of large nucleation stimulating particles only randomizes the texture to a limited extent.

2.4. Calorimetric studies of recrystallization

(In collaboration with the Physics Department at Risø)

The stored energy in a deformed material is released during annealing at sufficiently high temperatures. This energy acts as the driving force for both recovery and recrystallization processes. Thus valuable information can be obtained from measurements of the energy release during annealing by calorimetric techniques. Microcalorimetric measurements were used to study the recrystallization process of two materials, pure Cu (99.9%) and commercially pure Al (99.4%), deformed by cold-rolling to 95% and 90% reduction in thickness, respectively. The energy stored on deformation was determined from an integral over the energy released by heating the sample at a constant rate. The

corrections for the specific heat background were performed by subtraction of an identical measurement on the recrystallized sample. The energy stored in the samples were 56.9 J/mole for Cu and 21 J/mole for Al.

The recrystallization kinetics of the Cu-material was studied by measuring the power release as a function of time under isothermal conditions at six temperatures between 420 K and 470 K. The energy released at time t was determined and analysed on the basis of a simple Avrami type equation. From the measurements the activation energy $Q = 129$ kJ/mole was determined from the temperature dependence of the relaxation times. Analysis of neutron diffraction texture measurements on materials given the same pretreatment gave an activation energy of $Q = 113$ kJ/mole. The Avrami β -values, which relate to the recrystallization morphology, were found to be in the range from 0.9-1.6 as in the neutron diffraction studies. However, because absolute values of relaxation times were found in striking disagreement, measurements by the two techniques should be performed on samples from the same batch.

2.5. Small angle neutron scattering study of γ' -precipitation (In collaboration with Hahn-Meitner Institut für Kernforschung, Berlin)

To obtain a basic understanding of γ' -precipitation in nickel-base super alloys, the coarsening kinetics of the γ' -precipitates was studied in a model system (Ni with 12 at % (Al, Ti)) by small angle neutron scattering (SANS). A Guinier analysis of the measured SANS data was made in order to determine the average particle size in a series of samples annealed for various times at temperatures between 773 K and 873 K. The average shortest interparticle distance was estimated from the position of the peak-intensity. By log-log plots of the interparticle distances and the particle radii versus annealing time information about kinetics is obtained. It was found that at the higher temperatures (> 823 K) the data follow the kinetics predicted by

dicted by classical diffusion controlled coarsening. An analysis of the kinetics at the lower temperatures is in progress.

2.6. Creep in fcc metals

Specimens of Al-11% Zn were deformed in creep at 250°C under stresses in the range 8 to 12 MN/m². The dislocation structures in the deformed specimens were examined by transmission electron microscopy; in particular the sub-boundary structure was studied. An example of a dissolving sub-boundary is shown in Fig. 2.



Fig. 2. Dissolution of a sub-boundary in creep-deformed Al-11% Zn.

2.7. Plastic deformation of composites

The mean field theory for composites was applied in a comprehensive analysis of available tensile data for the copper-tungsten system. In the case of particle composites the theory overestimates the measured overall elastic stiffness. The overestimate is attributed to deviations from ideal behaviour. It seems likely that the measured strain includes some preferential yielding caused by local thermal residual stresses at the particles. Interface sliding or decohesion is less likely, because the composites display very high ductilities, much higher than that of the free particles. The observation of high ductilities was discussed in terms of two physical models: in the continuum model the constrained plastic deformation of the matrix around non-deforming particles cause dislocation accumulation and hardening of the matrix. This leads to an overall workhardening rate of the composite which increases more rapidly with decrease of particle diameter than does the overall flow stress. It follows from the Considère criterion that a decrease of the particle diameter increases the uniform elongation. In the isostrain model, on the contrary, it is assumed that the hydrostatic compression of the particles due to thermal residual strains enhances their ductility, thus allowing compatible deformation of the composite to large plastic strains.

In the case of fibre composites tensile data is available as "derived matrix curves", i.e. the in-situ flow stress in the matrix versus the total strain of the composite. The data cover fibre diameters ranging from 10 μm to 230 μm in hot pressed systems (polycrystalline matrices) or liquid infiltrated systems (single crystal matrices). Given information on stress relaxation rates the mean field theory allows the calculation of curves of in-situ flow stress τ versus plastic strain e_p in the matrix. Figure 3 summarises the in-situ workhardening rates, $\theta = \partial\tau/\partial e_p$, calculated from such curves for an assumed stress relaxation rate of 2/3. There is for both systems a strong increase of θ with increase of the fibre volume fraction, f . The value of θ approaches the shear modulus of the matrix when f approaches ~ 0.5 . Increase of the fibre diameter, d , decreases θ ,

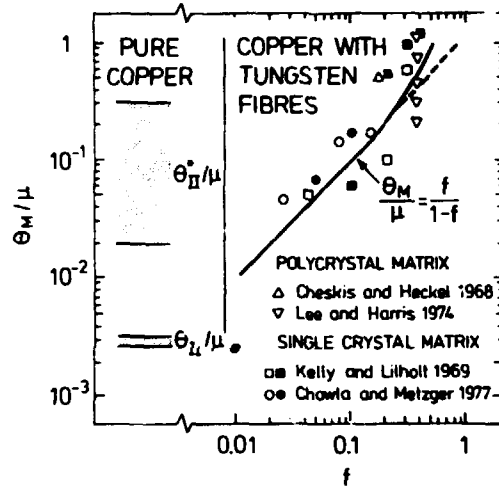


Fig. 3. Summary of the in-situ tensile matrix hardening rates derived on the basis of the mean field model from experimental data on copper-tungsten fibre composites.

particularly in the hot pressed system. The matrix hardening was discussed in terms of two models: according to the residual stress model the in-situ flow stress is a linear combination of the applied stress and the unrelaxed plastic strain in the matrix. The coefficients in the linear combination depend on f but not on d . Consequently, according to the residual stress model, the observed fibre diameter dependence of hardening must be associated with the rate of stress relaxation rather than with the hardening mechanism itself. On the other hand, differential thermal shrinkage during fabrication generates dislocation substructures in the matrix. According to the matrix substructure model this should, at least in some cases, account for the matrix hardening.

2.8. Fatigue in metals

Hardening diagrams were developed for copper polycrystals from theory and experimental observations in constant plastic strain amplitude fatigue. According to a comprehensive computer model for the quasi-monotonic plastic deformation of polycrystals (section 2.9) there is a transition from single to multiple slip at an overall plastic strain of the order 10^{-3} . This is consistent with the observation that cyclic deformation at constant plastic strain amplitudes ϵ_{pa} leads to dislocation microstructures involving secondary dislocations if $\epsilon_{pa} > 10^{-3}$, while pri-

primary dislocations dominate when $\epsilon_{pa} < 10^{-3}$. These two regimes can be seen in the hardening diagram. As in single crystals the observations suggest that there is a succession of stages of primary slip, fields I, II* and III*, followed by a stage of multiple slip, field III. Primary slip in field I appears to be enhanced by latent hardening of secondary slip systems: the initial cumulative hardening rate θ_{cum} of polycrystals exceeds that of single crystals by up to an order of magnitude. This excess hardening may be attributed to the intergranular stresses imposed by primary slip, as described in the Sachs model. With continued cycling primary veins nucleate, at the transition to field II*, and grow until thin PSBs nucleate at the transition to III*. Through III* the PSBs gradually evolve into the cells characterizing field III. The hardening diagrams may be used in interpreting variable plastic strain amplitude fatigue, as indicated by the strain paths in Fig. 4.

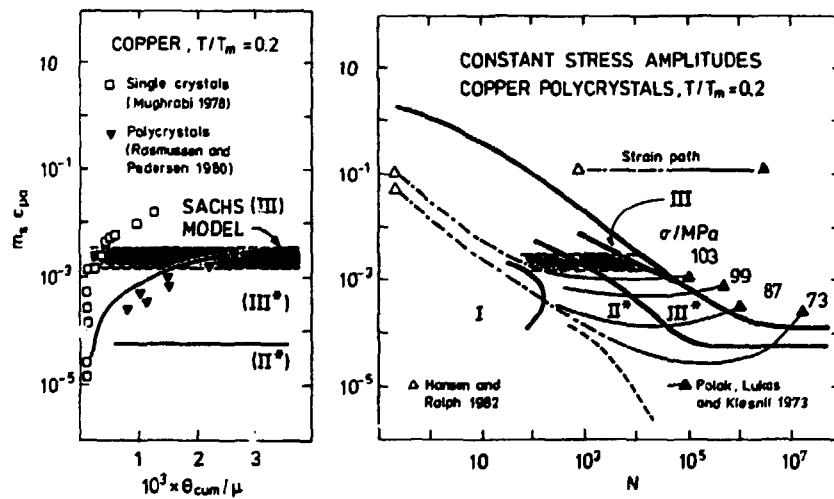


Fig. 4. Application of the hardening diagram for polycrystals in the interpretation of constant stress amplitude fatigue. Cyclic deformation at constant plastic strain amplitude in field I is associated with high intergranular stresses imposed by primary slip in individual grains, as described in the Sachs model.

Experimental studies of fatigue of copper single crystals were continued in collaboration with the Cavendish Laboratory, Cambridge University. Single slip oriented single crystals of copper were cyclically strained at room temperature into fields II* and III* and examined by transmission electron microscopy. The aim is mainly to examine whether the nucleation of PSBs can be described in terms of a composite model in which veins do not normally deform plastically.

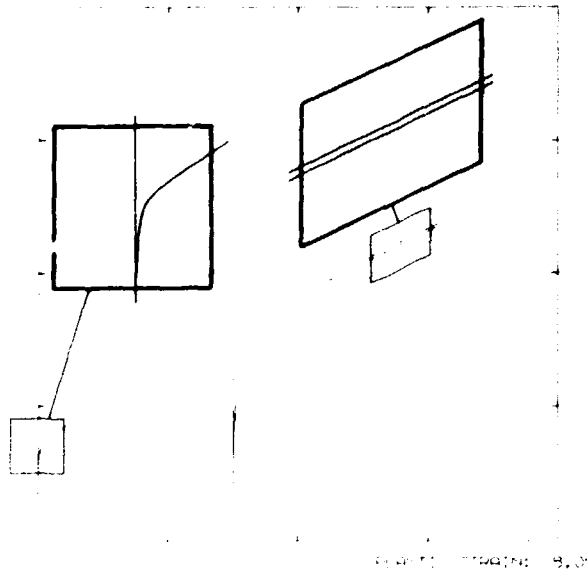


Fig. 5. Stress-strain curve up to 6 per cent strain with work hardening and Bauschinger experiment (strain reversal at 3 per cent). 100 grains, 1600 Q₂₂ steps.

2.9. Plastic deformation of polycrystals

A new comprehensive computer model for the plastic deformation of polycrystals was developed. It includes the elastic-plastic transition together with texture evolution and work hardening of the individual grains. The model is also capable of reversing the direction of strain and stress, i.e. of performing a Bauschinger experiment. Permanent softening is observed in such computer Bauschinger experiments, see Fig. 5.

The deformation patterns in fine-grained (50 μm) and coarse-grained (300 μm) commercial aluminium were compared for rolling up to 95% reduction. The evolution of surface slip markings and bulk structure with strain was rather similar in fine-grained and coarse-grained material - with a trend for the structural evolution to be slower in coarse-grained material. The evolution in texture, on the other hand, was quite different in the two materials: in the fine-grained material there was a normal development towards a rolling texture from the initial stage of deformation, whereas the initial texture in the coarse-grained material (practically identical to that in the fine-grained material) had a remarkable stability up to about 50% reduction.

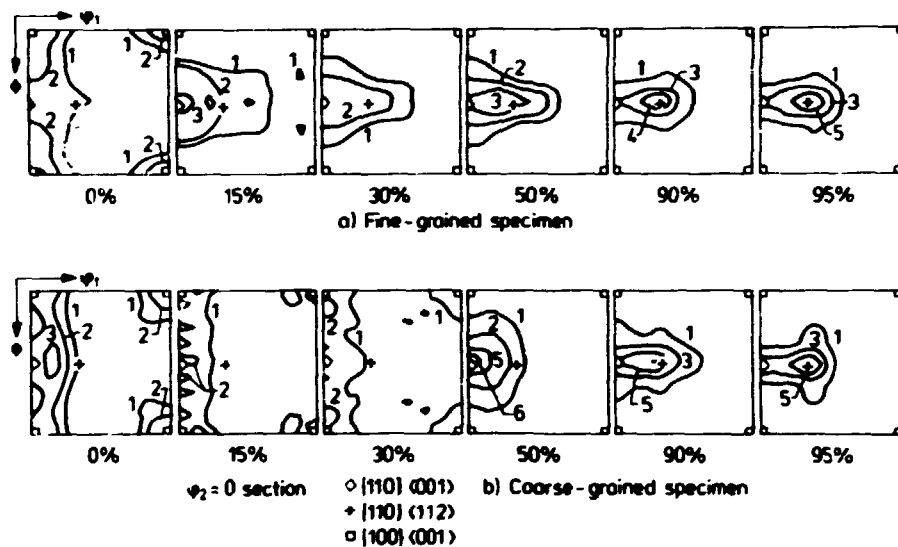


Fig. 6. ODF-sections ($\phi_2 = 0$) for coarse-grained and fine-grained specimens of aluminium (99.6 per cent) from the undeformed state to 95 per cent reduction in thickness by cold rolling. The figure illustrates the significant effect of the initial grain size (300 and 50 μm) on the texture development during cold rolling.

The heterogeneities developing with monotonic strain in extremely coarse-grained aluminium (1.5 mm in grain size) were investigated. Scanning electron microscopy (channelling contrast and selected area channeling patterns) revealed that the grains fragmented into differently oriented domains; in material with 5% tensile strain orientation differences of up to 6° were observed within individual grains. Considerable variations in microhardness within the grains and between the grains were also observed. The level of heterogeneity was about the same in the surface and in the bulk (several grain diameters away from the surface).



Fig. 7. Strain induced fragmentation of large grains in aluminium into differently oriented domains, as revealed by channelling contrast microscopy.

2.10. Irradiation of high-purity aluminium with 600 and 800 MeV protons

(In collaboration with EIR/SIN, Würenlingen, Switzerland and Los Alamos National Laboratory, Los Alamos, U.S.A.)

High-purity aluminium (99.9999%) samples were irradiated with 600 MeV protons at the Swiss Institute for Nuclear Research (SIN) to different dose levels (up to 5 dpa) at temperatures in the range 120-430°C. In an attempt to obtain information about the helium bubbles produced during 600 MeV irradiation, the samples irradiated at 120, 140 and 430°C were investigated by the positron annihilation technique. In the samples irradiated at low temperature, changes in the lifetime of trapped positrons with dose and temperature are correlated with the bubble size. The density of helium atoms in the bubbles is estimated to be $7 \pm 14 \times 10^{22} \text{ cm}^{-3}$. The samples irradiated at 430°C exhibited an unusually narrow component of the angular correlation curve associated with positronium formation in the bubbles, probably a result of segregation of transmutation produced Na at the bubble surfaces. The sample irradiated at 430°C was studied with small-angle neutron and X-ray scattering techniques (SANS and SAXS). The size distribution of helium bubbles obtained from scattering measurements and TEM were found to be in good agreement. However, a noticeable difference in the X-ray and neutron scattering was observed, the difference could not be directly related to the helium content in the bubbles. Instead, the difference may be related to other impurities such as Mg provided they segregate near the bubble surface.

High-purity aluminium samples were also irradiated with a pulsating beam of 800 MeV protons at Los Alamos National Laboratory. The sample temperature during irradiation was calculated to be between 50 and 100°C. Nine weeks of irradiation gave a displacement dose of about 0.5 dpa. These specimens were studied with the SANS technique; SANS measurements clearly indicate the presence of a dense population of small cavities in the irradiated specimens.

2.11. Accumulation of gas atoms at grain boundaries during irradiation

(In collaboration with Metallurgy Division, AERE Harwell, U.K.)

The production of helium and hydrogen is relatively fast in the structural materials used for fusion devices. At elevated temperatures helium can accumulate at grain boundaries and can cause embrittlement. The rate at which gas will accumulate on grain boundaries during irradiation depends upon the nature of the sinks for gas (e.g. voids or bubbles) within the grains, since the gas being produced must be divided between the grain and grain boundary. An analytic calculation was made to determine the flux of gas atoms to a planar boundary under conditions of uniform gas production. Each grain is assumed to contain a uniform density of bubbles of a certain size and with a bubble denuded zone of a certain width on each side of the boundary. The

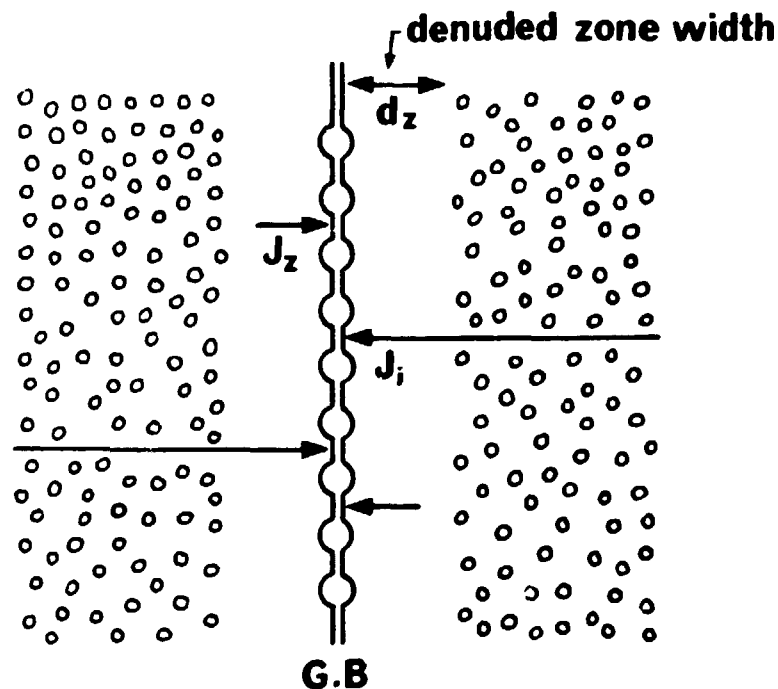


Fig. 8. Schematic representation of the analytical model used to estimate the flux of gas atoms to a grain boundary from denuded zones and grain interiors.

flux was calculated as a function of the size and density of the bubbles in the grain interior and the width of the bubble denuded zone adjacent to the boundary. In the calculation no account is taken of possible spatial variations in the gas diffusivity, as might occur as a result of impurity-segregation, etc.

The validity of the gas diffusion calculations can be tested since the gas accumulated on grain boundaries is contained in bubbles which can be observed by TEM. The size and density of bubbles at grain boundaries was determined for aluminium irradiated with 600 MeV protons at 413, 443 and 493 K. The gas content of the boundaries is then estimated using the helium equation of state. The calculated helium content of the grain boundaries is found to be in very good agreement with the experimentally measured values. The calculations demonstrate how the gas flux to the grain boundaries can be influenced by the density of bubbles in the grains. By producing a very high density of gas bubbles in the grain interior, as is likely to be the case when gas generation rate is high, one can reduce substantially the accumulation of gas at the grain boundaries, with a possible reduction in the embrittlement.

2.12. Nucleation and growth of microstructural inhomogeneity during irradiation

(In collaboration with FPTI Kharkov, U.S.S.R and R.R.C Kalpakam, India)

Since the displacement damage produced during irradiation is spatially homogeneous, it is commonly assumed that the evolution of dislocation and void microstructure would occur also in a homogeneous fashion. Experimental results have demonstrated, however, that during low dose ($1-5 \times 10^{22}$ n/m²) neutron irradiations (in DR 3 at Risø) of high-purity copper at 250°C ($0.39 T_m$) the irradiation induced vacancies and self-interstitials cluster mostly as "walls" of dislocation loops and segments, the concentration of dislocation loops and segments between these walls being very low. The vacancies also precipitate inhomogeneously: voids are observed only in the region

between the walls and not within the walls. Furthermore, a zone along the dislocation walls is completely denuded of voids. In specimens irradiated to 5×10^{22} n/m², the total dislocation density in the well-developed walls was estimated to be $\sim 10^{14}$ m⁻²; the dislocation density between the walls was very low ($\sim 10^{11}$ - 10^{12} m⁻²). The inter-wall spacing varied between 2 and 10 μ m and the wall thickness varied between 0.05-0.5 μ m. The average void density and size in these specimens were found to be 1×10^{20} m⁻³ and 17.1 nm, respectively. Assuming zero incubation dose, these void parameters would give a swelling rate of $\sim 2.5\%$ dpa⁻¹.

The observations on the nucleation and growth of inhomogeneous and segregated microstructure during irradiation of copper are consistent with the results on high-purity aluminium (99.9999%) irradiated with fast neutrons in DR 3 reactor at Risø. The aluminium samples were irradiated at 120°C (0.39 T_m) to different doses in the range 2×10^{21} - 5×10^{24} n/m². In the aluminium samples polygonized dislocation walls were introduced prior to irradiation by cold-working and annealing. As in Cu, no voids were formed within the dislocation walls and there was a well-defined void denuded zone along the walls. In specimens irradiated up to 1×10^{24} n/m² the average swelling rate for the region between the polygonized walls was $\sim 2\%$ dpa⁻¹; the total dislocation density in this region was quite low ($\sim 2.5 \times 10^{12}$ m⁻²).

In an attempt to understand these observations the effect of heterogeneous sink distributions on void swelling was evaluated quantitatively using the standard rate theory concept. The calculations demonstrate that neither the high swelling rate nor its spatial variation can be explained in terms of the commonly assumed process of preferential absorption of randomly diffusing self-interstitials to dislocations. It was argued that in order to explain the high swelling rate in the presence of a very few dislocations, it is necessary to consider the mechanism(s) that can provide more efficient removal of self-interstitials. In principle this can be achieved by postulating either that the voids have a positive bias for vacancies or that the self-interstitials are transported by a mechanism other than three-dimensional random diffusion.

In order to understand the growth of microstructural heterogeneities during uniform irradiation conditions, an analytic model based on the rate theory approach was considered. The analysis shows that the structure of the rate equation is such that any inhomogeneity in the microstructure tends to be enhanced rather than suppressed. The point defect diffusion flux the inhomogeneity produces, leads to its further spatial growth. The spatial growth saturates when the sink density becomes sufficiently high to that point defect absorption essentially inhibits diffusion. The analysis shows that the scale of growth of inhomogeneity will be determined by the inverse square root of the dislocation density.

2.13. Quasielastic neutron scattering studies of the ionic conductors $\text{Ba}_{1-x}\text{U}_x\text{F}_{2+2x}$

(In collaboration with the Physics Department at Risø)

The fluorine ionic conductors $\text{Ba}_{1-x}\text{U}_x\text{F}_{2+2x}$ crystallize in the fluorite type of fcc structure. The process of ionic conduction is established by defects in the lattice generated thermally as Frenkel pairs or by doping. The defect structure of $\text{Ba}_{1-x}\text{U}_x\text{F}_{2+2x}$ ($x=0.02, 0.05$ and 0.15) was studied by quasielastic neutron scattering. At room temperature the diffuse scattering was measured in the plane spanned by $(1,0,0)$ and $(0,1,1)$ for wave-vector transfers up to 3 \AA^{-1} . The diffuse patterns were qualitatively similar for the three UF_4 concentrations, indicating a concentration independent defect structure. The scattering was elastic within an experimental resolution of 0.7 meV . The diffuse pattern was analysed by model calculations based on different defect clusters. Good agreement between measured and calculated patterns was obtained with a simple 212 -cluster configuration (two F^- interstitials, one U^{4+} and two relaxed F^-) but improvements were observed if small additional relaxations of the fluorine ions around U^{4+} were allowed. The stability of a trimer cluster configuration (one U^{4+} , one F^- vacancy and three F^- interstitials), which has been advanced recently on the basis of lattice defect calculations, could not be verified from our diffuse neutron scattering studies. Preliminary studies of

the diffuse pattern along the main symmetry directions as a function of temperature suggest that dynamical defect clusters similar to those observed in undoped fluorites are formed at high temperatures.

2.14. Oxygen conductors and electrode materials for fuel cells

The materials research in this project will be directed towards a thorough characterization of the properties of potential oxygen conductors for fuel cells and similar electrochemical systems. The techniques available for these studies comprise: a 4-probe setup for ac-impedance measurements in controlled atmosphere at temperatures up to 1500°C; a least-square fitting programme for evaluation of impedance plots; X-ray, electron- and neutron diffraction for characterization of the defect structure; thermal analysis, techniques comprising thermogravimetry, differential thermal analysis (DTA) and differential scanning calorimetry (DSC) and dilatometry. Measurements were initiated on gadolinia doped uria using these techniques.

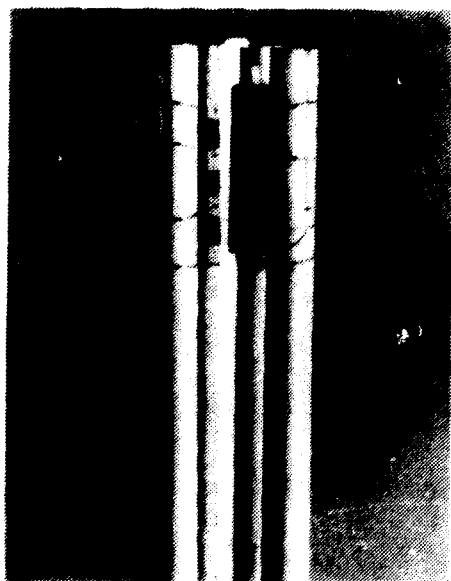


Fig. 9. Alumina sample holder for four-probe ac-impedance measurements on oxygen conductors. Four samples can be measured simultaneously.

3. TECHNOLOGY AND MATERIALS DEVELOPMENT

The materials technology programme concentrates on the development of new materials and methods for their fabrication, characterisation and testing. Projects related to alternative energy technology include work on the mechanical properties of fibre reinforced plastics for light and strong components, e.g. wind-mill blades (3.5-3.6), work on metal-hydrogen systems for transportation and storage of energy (3.7), and work on materials for battery applications (3.8-3.9). Most of these projects are carried out in collaboration with the industry, partly under the auspices of EEC, the Nordic Fund for Industrial Development and the Ministry of Energy. Work on high temperature corrosion in conventional energy technology (3.4) is carried out within the European COST-501 project. This work is done in collaboration with a Danish firm and partly sponsored by the Ministry of Energy. In the area of non-destructive testing (3.12) the work is concentrated on quantitative ultrasonic examinations, especially the characterization of materials and sound fields. Further projects are centered on the development of materials and processes, including ceramics for measurement of oxygen potentials in combustion gases (3.10-3.11), sintering of nuclear ceramics, and brazing technology (3.3). In the field of radiography standardization work is carried out (3.12) within the neutron radiography working group sponsored by Euratom. Due to their proprietary nature, some of the projects in the technology programme are excluded from the progress report.

3.1. Fatigue testing

Equipment was developed for studies of corrosion fatigue at constant or variable amplitudes in off-shore steels. An off-shore steel (St 52,3) was fatigue tested at constant plastic strain amplitudes in air. Optical and electron microscopy were used to examine the surface and bulk microstructures in the fatigued

specimens. High frequency fatigue tests were performed using a newly installed Instron 1603 electromagnetic resonance machine. The materials tested were used in the EEC sponsored project "Silver-Saving by Substituting Brazing Alloys with CuP Alloys". Constant amplitude fatigue tests were performed on specimens of glass fibre reinforced plastics with constant interrupt intervals for measuring static stiffness. Equipment was developed for fatigue pressure vessels made of fibre reinforced plastics.

3.2. Fracture testing

The collaborative IAEA programme on "Analysis of the Behaviour of Advanced Pressure Vessel Steels under Irradiation" was completed. The programme involved the testing of specimens subjected to various doses of neutron irradiation. Testing and analyses were carried out according to the multispecimen J-integral based resistance curve procedure. Only modest influence of irradiation was seen. Testing of fracture toughness and acoustic emission within a programme carried out for the European Coal and Steel Communities was completed. A review was given of the general characteristics of acoustic emission signals during the deformation and fracture of metals as well as of the parameters most often used in the description of these signals. Activities in the area of dynamic fracture mechanics were resumed. Crack arrest properties were measured in a variety of steels (ASTM collaborative programme) and specifically in steels for off-shore application (programme sponsored by the Ministry of Energy).

3.3. Brazing and soldering

Testing was continued to evaluate the resistance to corrosion in 1-3% HNO_3 at 80°C of joints in 18/8 stainless steel. The joints are made using Ni-Cr based brazing filler metals. Investigations of a wide range of these filler metals suggest that a Cr content well in excess of 20% is needed to give the required corrosion resistance under production conditions. Contract work was continued on industrial applications of dip brazing, vacuum brazing and ultrasonic soldering of aluminium as well as vacuum brazing of stainless steels, aluminium alloys, super alloys and titanium.

3.4. High temperature corrosion

(In collaboration with A/S Haldor Topsøe)

A special form of carburization, the so-called metal dusting, was studied with the purpose of getting a better knowledge of the conditions under which metal dusting occurs and of the relative susceptibility of a number of alloys to this form of deterioration. A number of alloys (low alloy and high alloy steels and nickel base alloys) were exposed to atmospheres (mixtures of H_2 , CH_4 , CO and H_2O) of carbon activity one and being reducing against iron oxides but oxidizing against chromium, at temperatures of 400°C , 500°C , 700°C and 800°C . Chromia formed on the surface protected the alloys and no metal dusting was observed, under these conditions. In further experiments atmospheres which are reducing against chromia will be used as well as atmospheres which periodically changes between being reducing and oxidizing. The experiments were carried out as part of the European COST 501 programme. Contract work was continued on problems concerning industrial applications of high temperature materials (oxidation, carburisation, sulfidation, nitriding etc.).

3.5. Fibre reinforced plastics

Research and development on fibre reinforced plastics were continued in the following fields: fabrication technology, testing methods, mechanical properties and design and analysis. Development of the computer controlled filament winding machine was continued. The software was improved to ensure more accurate positioning of the fibre, and a more easy teach-in procedure for new winding patterns on complicated mandrels. The hardware was expanded with an oven, so that the temperature in the box where the filament winding is placed can be controlled, to ensure correct viscosity of the matrix. Among other applications the filament winding machine was used to fabricate pressure vessels and tubes of fibres with high bending stiffness of fibre reinforced plastics. A paddle for a kajak of carbon fibre reinforced epoxy was manufactured in our autoclave to obtain experience with double curvature sandwich constructions.

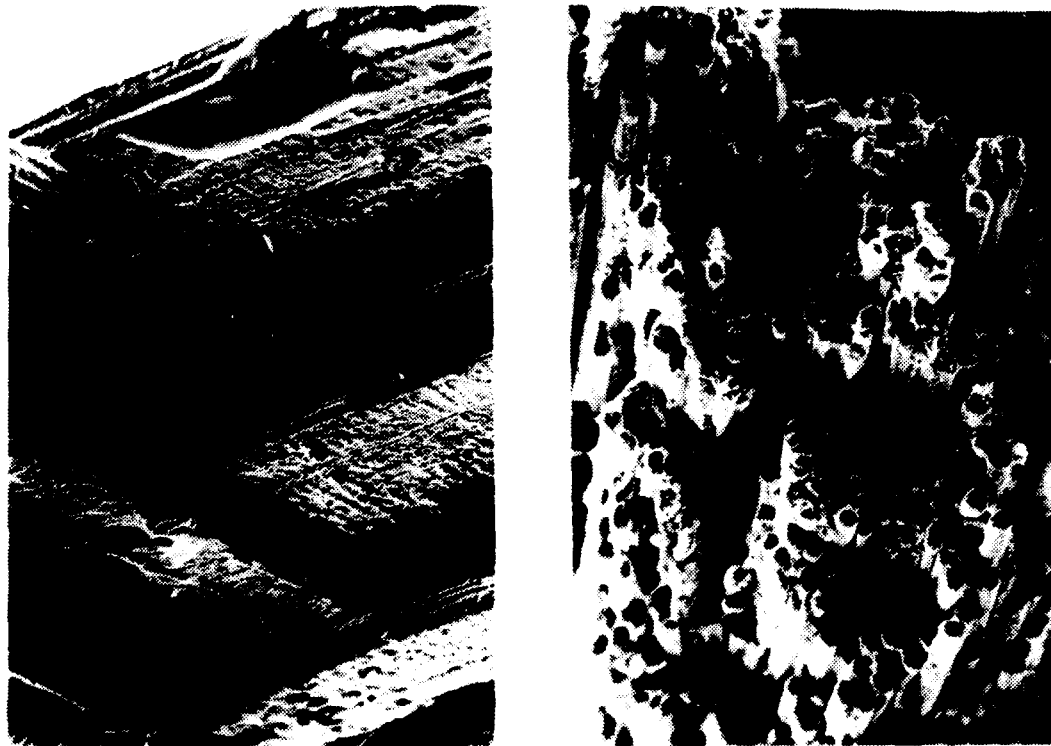


Fig. 10. Fracture of a carbon/epoxy laminate with fibre orientations of -45 and $+45$ degrees. Ends of broken carbon fibres are shown.

3.6. Damage in laminates

Work on damage in angle-ply laminates is carried out to study the influence of fibre orientation, stacking sequence and specimen geometry on the damage development and strength. To study failure mechanisms replicas are taken of the free edge of carbon/epoxy tensile specimens at different strain levels, the edge is examined in an optical microscope and X-ray photography is used together with a contrast liquid to reveal interior cracks or delamination. Scanning electron microscopy is used for examination of the damage zone after ultimate failure. The tensile specimens are cut from plates cured in an autoclave. To ensure that the specimens are without initial damage the plates are examined by ultrasonic C-scan and the edges of the specimens are examined by X-rays and contrast liquid.

3.7. Metal-hydrogen systems

Investigations of the energy storage potential of magnesium/magnesium hydride were continued on a 2 kWh storage tank system. The magnesium powder reacted consistently with 75-80% of the theoretically possible amount of hydrogen at the applied temperature/pressure conditions (350-400°C/2-3 MPa). During desorption all the absorbed hydrogen was released. The absorption and desorption rates are easily controlled for effects up to approximately 20 kW. The reaction kinetic is seriously reduced only close to full absorption or desorption.

It is at present not understood why 20-25% of the charge is inactive. Even at prolonged exposure to hydrogen at thermodynamically favourable conditions the overall degree of reaction is not increased. A possible explanation is that the powder is compacted so densely during the 20% volumetric expansion associated with the hydrogenation that some regions are inaccessible to hydrogen. However it is more likely that the reaction of the largest particles is incomplete. From past experience we know that particles larger than approximately 75 μm diameter are not fully converted to hydride. In the applied

Mg-powder about 1% of the particles, equivalent to 15-20% of the powder mass, exceeded this size. A charge of the same powder, with particles of size above 65 μm removed, was prepared and will be tested under conditions identical to those for the unfractionated powder.

A project aiming at assessing the hazards of magnesium hydride was started. No experimental data are available for the hydride combustion (ignition parameters, dust explosivity, fire extinguishing rates) nor for the alleged dangerous reaction with water. From a purely energetic point of view the hydride should be more hazardous than the metal, since the total combustion energy is higher, 770 kJ mol^{-1} compared with 600 kJ mol^{-1} . Preliminary experiments, however, show that the kinetics are in both cases much slower and consequently the hydride generally safer to handle. The explanation is related to the release of hydrogen. This requires a substantial amount of energy and consequently lowers the temperature and at the same time it constitutes a barrier to the air. On the basis of the preliminary experiments fully monitored combustion and water reaction test are in preparation.

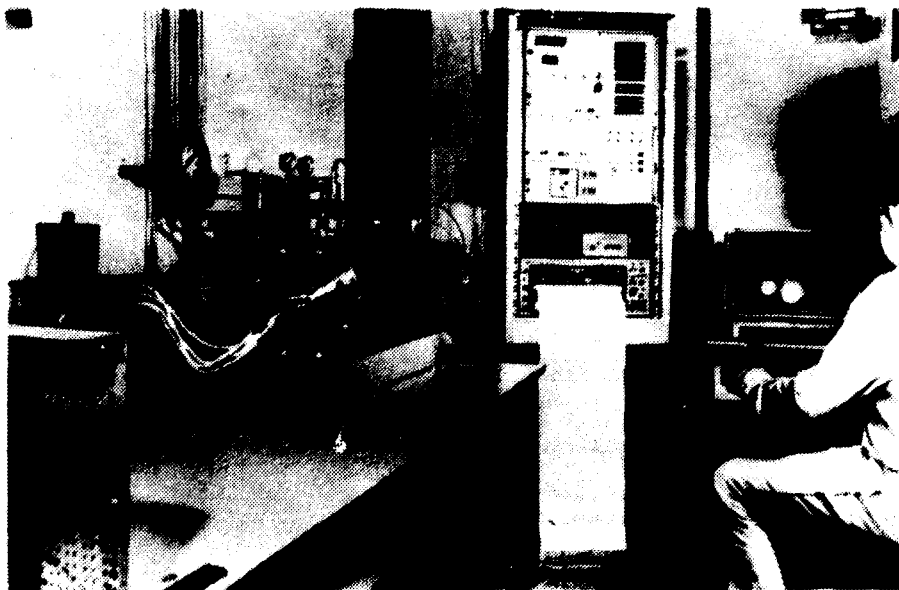


Fig. 11. A 2 kWh hydrogen storage tank containing up to 800 g magnesium powder in four cylindrical cartridges. Temperature and pressure monitoring facilities and control panel can also be seen.

3.8. Lithium electrodes for non-reversible batteries

(In collaboration with A/S Hellesens)

Studies were continued on the formation of a passivating LiCl-layer on the lithium anode in non-reversible lithium-thionyl-chloride batteries. Lithium metal is stable in SOCl_2 solutions due to the formation of a passivating layer of LiCl at the Li- SOCl_2 interface. A similar layer is formed on other metals in case these are in contact with lithium. These passivation phenomena are of great importance in the context of the Li- SOCl_2 battery performance because the LiCl is the solid electrolyte separating the active components of the cell. The formation and growth of the LiCl film takes place gradually, the Li-electrode being covered by a Li_2O film before exposure to the SOCl_2 electrolyte. The properties of the electrode surface were studied by means of ac-impedance measurements during the formation and growth of the LiCl-layer. The effect of the following electrolyte parameters were investigated: impurity level, acidity, SO_2 content and temperature.

3.9. Solid electrolyte research

Lithium-, sodium-, and potassium ion conducting solids were synthesised and characterised by impedance spectroscopy, X-ray/neutron diffraction, and thermochemical methods. Highly conducting materials (single phase and composite type) were studied with special emphasis on surface and structure enhancement of the conductivity. Several materials were studied in the "super ionic" state. A facility for fabrication and manipulation of thin films (50-2000 nm) of lithium metal, lithium alloys and alkali metal ion conductors was installed, see Fig. 12. A computer controlled, sensor surveyed glove box system was built around a vacuum deposition chamber for this purpose. Experiences in making thin film lithium batteries and sensor devices based on thin films were obtained.



Fig. 12. The newly installed facility for fabrication and manipulation of thin films of lithium metal, lithium alloys and alkali metal ion conductors.

3.10. Oxygen conductors

Oxides with a high ionic conductivity for oxygen are of interest as electrolytes for oxygen sensors, fuel cells and membranes for gas separation. Hitherto these systems have been based mainly on doped zirconia, which, however, require a high operating temperature due to their relatively low ionic conductivity. With the aim of developing new oxygen conductors with higher ionic conductivity, which would reduce the required operating temperature, the ceria-gadolinia system were examined. Methods for fabrication and characterization of test specimens of ceria-gadolinia solid solutions were developed. The fabrication methods comprise: homogeneous coprecipitation of carbonates by hydrolysis of ceria, calcination, ball milling, pressing (discs and tubes) and sintering in air. Specimens were characterized by X-ray diffraction (structure), emf measurements, dc- and ac conductivity measurements, scanning electron microscopy (Gd-distribution) and thermogravimetry (chemical and thermal stability). The results obtained can be summarized as follows:

- a) Specimens with a high density and a homogeneous distribution of Gd can be prepared by the fabrication route developed.
- b) These specimens, which can be prepared for any composition in the ceria-gadolinia system, showed an excellent chemical and thermal stability.
- c) The highest dc-conductivity was obtained for the composition CeO_2 -8 mole % $\text{GdO}_{1.5}$.
- d) The 2-probe ac-impedance measurements showed that the total conductivity below 650°C is dominated by grain boundary conduction for the specimens containing 10 mole % $\text{GdO}_{1.5}$ whereas lattice conduction dominated in the specimens containing 30 mole % $\text{GdO}_{1.5}$. For specimens with 50 mole % $\text{GdO}_{1.5}$ or more grain boundary conduction could not be determined.
- e) From 10 mole % $\text{GdO}_{1.5}$ and upwards the lattice contribution to the conductivity decreases with increasing Gd-content. This decrease corresponds to an increase in the activation energy for migration of oxygen. Fig. 13 shows the conductivities and activation energies determined for these oxides.

A major effort will be devoted to developing techniques for preparation and characterization thin films of doped oxides and electrode materials for fuel cells. The effort will be concentrated on the rf-sputtering technique, which has the following advantages: it can be used to produce thin films of a large number of both ceramic and metallic materials; stable films with optimal adhesion can be obtained by etching the surface of the substrates prior to the film deposition; and the consumption of materials is very small which allows the use of expensive materials, e.g. noble metals for catalytic electrodes. An rf-sputtering system was designed and ordered. The system is expected in operation early 1985.

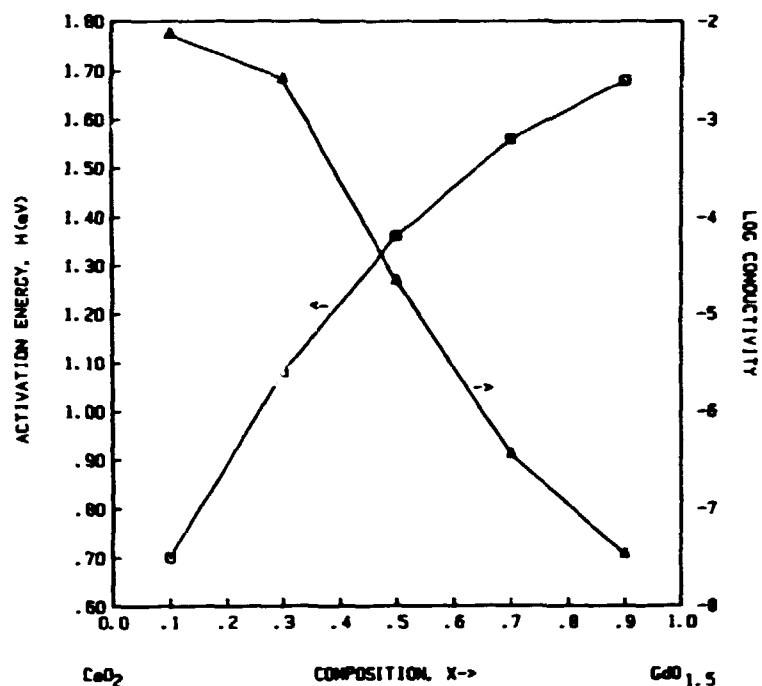


Fig. 13. Graph showing the activation energy and conductivity (at 500°C) of cerium-gadolinium oxygen ion conductors as a function of their composition.

3.11. High temperature oxygen-gas sensors

(In collaboration with A/S Oxydan)

For standard oxygen-gas sensors with porous Pt-electrodes the maximum temperatures for long term measurements are generally limited to 1000-1600°C. For many applications the sensors therefore have to be placed in a separate furnace which can lead to false measurements and which, in some cases, will give a considerable delay in the measurement of the oxygen pressure. The general aim of this project is first to evaluate the factors limiting the use of oxygen sensors at higher temperatures (up to 1500°C) and then to test the effect of various modifications of the standard sensor in order to improve its usefulness for high temperature measurements. A computer controlled test unit was constructed and a comprehensive test programme of standard sensors based on yttria doped zirconia was started.

3.12. Non-destructive testing

In the area of ultrasonic examination efforts were concentrated on the observation of internal structures and damage in thin (1 mm) plates of carbon or glass fibre reinforced epoxy or polyester. It was possible to reveal delamination and other kinds of damage in the plates using a computerized scanning system, as illustrated in Fig. 14. It was difficult (or impossible) to use the interface echo in the normal pulse-echo technique, so a technique involving double-through transmission in immersion was used instead. The plates were also studied by the pulse transmission technique whereby ultrasound is sent along the plate, with transmitter and receiver on the same side but about 50 mm apart. The waveform is stored and analysed and the frequency spectrum is used to characterize the internal structure and damage state of the material. This work was done in collaboration with the Technical University of Denmark.

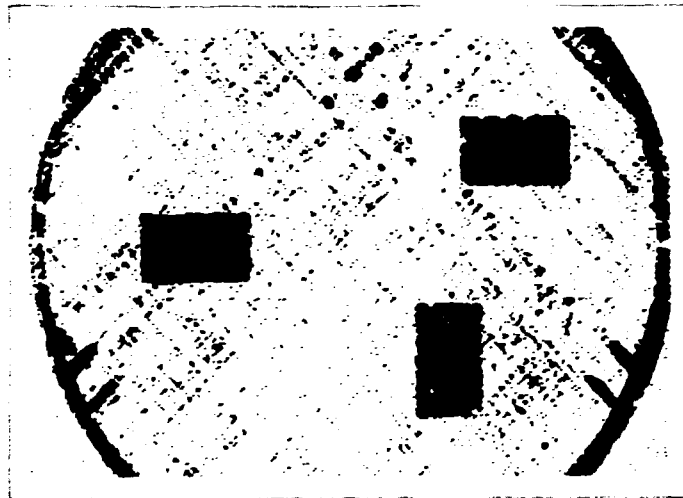


Fig. 14. Imperfections revealed in a plate of carbon-epoxy by the pulse-echo technique with computerized scanning.

The accuracy of eddy current techniques for measuring the thickness of thick (up to 1 mm) oxide layers on thin metal tubes (down to 0.15 mm) was determined using the lift-off technique. Different equipment was examined and the best suited was chosen for further experiments. This work was done under contract with the Joint Research Centre, Ispra.

The activity in neutron radiography was concentrated on the collaboration with the Euratom Neutron Radiography Working Group. Neutron radiographs of special indicators were collected and evaluated from centers participating in the work of the NRWG. The compilation of an EUR report on the use of nitrocellulose film and of the new edition of the Neutron Radiography Handbook were started. In the area of X-ray radiography investigation was performed on the newest brands of industrial X-ray films and radiographic paper designed for fast radiographic systems. Special X-ray film to be used with fluorometallic intensifying screens was compared with conventional fast X-ray films and radiographic paper exposed with fluorescent or fluorometallic screens. It was proved that in all instances radiographic image quality of at least 2% could be reached. The constant exposure technique was also used in the above comparison and proved very useful for that purpose.

4. FUEL ELEMENTS

The Danish water reactor fuels programme continues to utilize the irradiation facilities in the DR 3 materials testing reactor at Risø and the OECD Halden Reactor in Norway. Extensive post-irradiation examinations are performed in the Risø hot cells. An internationally sponsored three-year project, "The Risø Transient Fission Gas Release Project" is now well underway. This is a follow-up program to the "Risø Fission Gas Project" that was executed in 1980-81. Additional information on fuel performance becomes available from international collaboration arrangements, i.e. the OECD Halden Reactor Project (Norway), the "Super-Ramp" and "Trans Ramp" projects at Studsvik (Sweden) and Batelle's "High Burnup Effects Program" (USA). Outside these national and international programmes, valuable experience is gained from examination in the Risø hotcells, under special contracts, of foreign water reactor fuels. An important part of the current work comprises Pu-enriched fuel irradiated in the Italian Garigliano reactor up to 25,000 MWD/t.

4.1. UO₂-Zr irradiations

Standard fuel pins currently under irradiation in the DR 3 reactor have reached maximum burnup levels of 68,000 and 70,000 MWD/tU for BWR and PWR type fuel respectively. The irradiation facilities are also used for testing of LOWI duplex fuel (max. burnup 45,000 MWD/t, see also previous progress reports) and for transient tests with high-burnup fuel in the international fission gas project (see below).

The three Danish test fuel elements in the Halden reactor have now reached the following estimated burnups (average assembly, after correction for depletion):

IFA No.	165	201	202
MWD/tU	42,300	42,200	39,100

4.2. The Risø Transient Fission Gas Release Project

Late in 1982, a new international project was started, with the objective to study the kinetics of fission gas release in high-burnup fuel. The project period is three years and the sponsors are fuel suppliers, utility organizations, safety authorities and research organizations from Europe, United States and Japan.

Segments from previously irradiated $\text{UO}_2\text{-Zr}$ fuel pins are refabricated in the hot cells and mounted with pressure transducers. During transient testing in the DR 3 reactor at Risø, the change in internal pin pressure is monitored continuously. Before and after the transient testing, the fuel is characterized extensively in the hot cells.

Important test parameters in this project are: Transient power (up to 450-500 W/cm), burnup (13,000-50,000 MWD/tU) and fill gas (Xe, He at various pressures). Seven of the planned fourteen instrumented tests have been performed. In addition, two tests were executed with irradiated fuel pins that had not been opened in the hot cells (and consequently not instrumented), for comparison with the refabricated tests.

4.3. Continuous, on-line monitoring of internal fuel pin pressure

For the use in connection with fuel experiments in the DR 3 reactor new techniques were developed which allows the reconstitution of irradiated fuel, including monitors of a diaphragm pressure transducer. A number of experiments were performed which demonstrated excellent performance of the transducers as well as the fully computerized, measuring and data acquisition system. This system allows measuring of power and pressure in the experiments with high accuracy. Techniques were developed for the derivation

of gas release in fractions of the produced fission gas with overall accuracies better than 1% of the gas inventory. Releases down to 0.1% can be followed with a resolution in time of less than 1 minute.

4.4. Local gas release and swelling in UO_2 fuel during slow transient

The Metallurgy Department has an on-going cooperation with the Transuranium Institute in Karlsruhe, FRG, on the examination of transient tested water reactor UO_2 fuel. Examples of results from this work are given below.

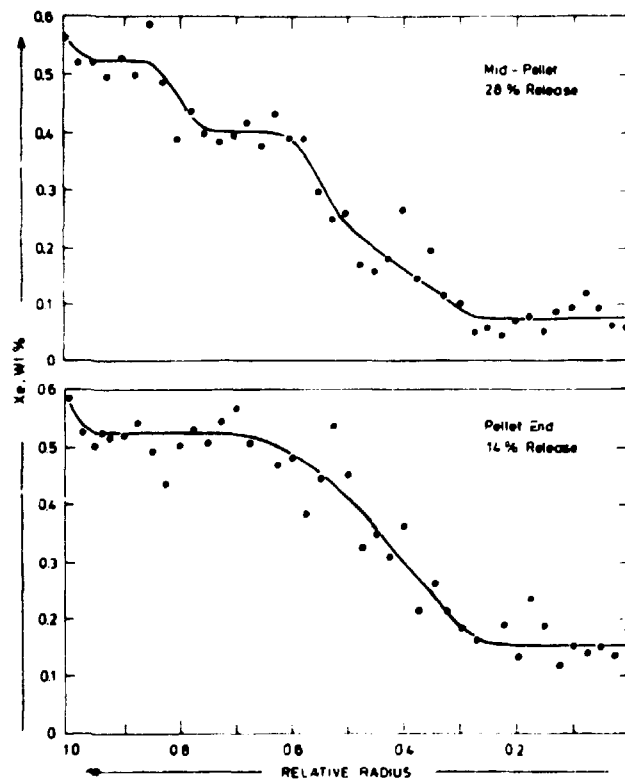


Fig. 15. Radial Xe concentration profiles in fuel sample P 14-6-56 taken from a transient tested pin. Test conditions: 295 W/cm for 72 h.

The concentration of fission Xe was measured on a longitudinal pellet section of a transient tested high burnup (37,300 MWD/tU) fuel by means of electron probe micro analysis. Fig. 15 shows the radial Xe concentration profiles at mid-pellet and at the pellet end. It was concluded that the pronounced difference is due to temperature differences, which can be referred to the fact that the pellet was dished and to the "bambooning" phenomenon.

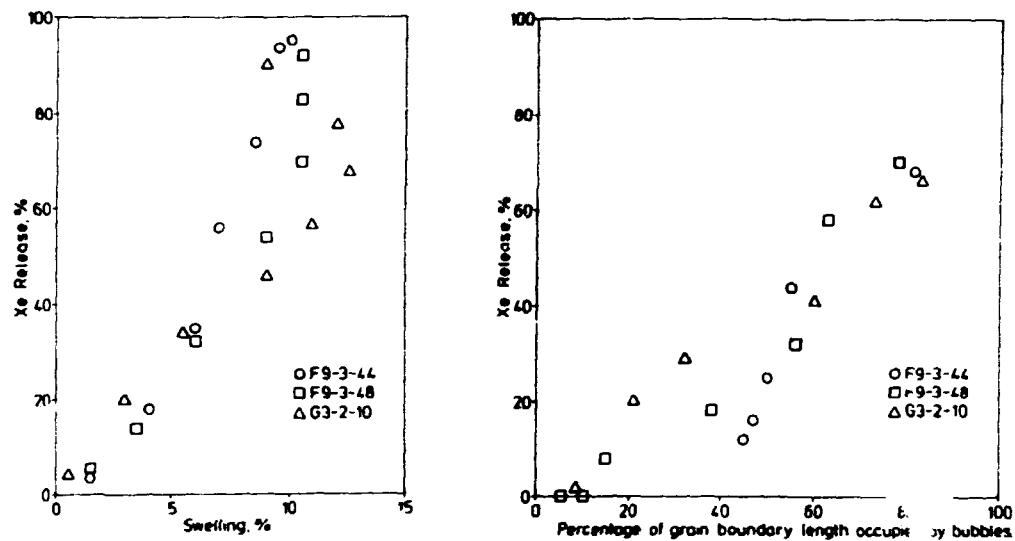


Fig. 16. (a) Xe release versus swelling for three transient tested fuel samples. Burnup from 3.7 to 4.3 per cent, test conditions: 380 to 415 W/cm for 24 h. (b) Xe release versus percentage of grain boundary length occupied by bubbles for the same specimen.

For other samples the local radial Xe release was correlated to the local swelling (including porosities down to 30 nm) and to the percentage of grain boundary length occupied by bubbles. The results are shown in Figs. 16a and b, and it is revealed that there is a continuous increase in both swelling and grain boundary porosity up to about 70% Xe release.

These observations indicate that the gas release during the 24 h transient was almost entirely controlled by grain boundary porosity formation and interlinkage, the Xe diffusion not being the release rate limiting factor.

5. PARTICIPATION IN INTERNATIONAL COLLABORATION

The department is engaged in the following types of international collaboration: joint research projects, committee work, reception of research fellows, and technical and scientific meetings.

The department was represented on the following committees:

The Information Exchange Group under the European Space Agency, on Carbon Fibre Reinforced Plastics,

The Halden Programme Group,

The IAEA International Working Groups on "Reliability of Reactor Pressure components" and "Water Reactor Fuel Performance and Technology",

The Super-Ramp and Trans-Ramp Project Committees, The Project Committee of the Batelle High Burnup Performance Programme (HEB), The Principal Working Group No. 3 (Primary Circuit Integrity) of the NEA Committee on the Safety of Nuclear Installations (CSNI),

The COST 501 Committee on Materials for Energy Conversion using Fossil Fuels,

The EEC Advisory Committee for Programme Management: "Plutonium and Transuranium Elements" and "High Temperature Materials",

The European Coal and Steel Community, Executive Committee No. 5: Failure Mechanisms and Design,

The Euratom Neutron Radiography Working Group,

The Council of the International Confederation of Thermal Analysis,

The Nordic Committee for Thermal Analysis,

The Technical Commission of the International Institute of Welding, Commission I, "Gas Welding and Allied Processes", Subcommission A, "Brazing and Surfacing",

Working Party for "Advanced Materials-Transport" of the CREST subcommittee for Raw Materials,

and The Fusion Materials Expert Groups of the European Fusion Technology Programme "Structural Materials" and "Breeding Materials".

6. EDUCATION AND TRAINING

N. Hansen and K. Rørbo gave regular lectures on materials science to students at the Danish Academy of Engineering. J. Bilde-Sørensen lectured in a course on "Methods for measurements on and characterization of surfaces" arranged by Danish Engineers' Post Graduate Institute (Danske ingeniørers Efteruddannelse). J. Bilde-Sørensen, N. Hansen, T. Leffers and H. Lilholt acted as external examiners at examinations for the Technical University of Denmark, O. Toft Sørensen acted as external examiner at examinations for the Technical University of Norway, Trondheim, and O. Bøcker Pedersen acted as official opponent in a disputation for the degree of dr. techn. at Tampere University of Technology, Tampere, Finland.

Post-graduate projects

Two post-graduate students from the Technical University of Denmark worked in the department on the following project in preparation for his licentiate (Ph.D.) thesis:

E.E. Salah Soliman	Grain Growth of Uranium Dioxide During Irradiation.
J.N. Andersen	Influence of small particles on the recrystallization texture of aluminium.

PUBLICATIONS

Metallurgy Department Progress Report for the Period

1 January - 31 December 1983

Risø-R-503 (1984) 72 pp.

The activities of the Metallurgy Department at Risø during 1983 are described. The work is presented in three chapters: General Materials Research, Technology and Materials Development, and Fuel Elements. Furthermore, a survey is given of the Department's participation in international collaboration and of its activities within education and training. A list (with abstracts) of publications and lectures by the staff during 1983 is included.

Microstructural Characterization of Materials by Non-Microscopical Techniques.

N. Hessel Andersen, M. Eldrup, N. Hansen, D. Juul Jensen, T. Leffers, H. Lilholt, O.B. Pedersen, B.N. Singh (editors).
Proceedings of the 5th Risø International Symposium on Metallurgy and Materials Science, Risø, 3-7 September 1984. (Risø National Laboratory, Roskilde, 1984) 605 pp.

The proceedings contain 10 invited papers and 64 contributed papers. Most of these papers deal with the application of non-microscopical techniques in the characterization of the microstructure of materials and the way this structure evolves during deformation, annealing or irradiation. The structural features covered include the total population of structural defects - not only point defects, cavities and dislocations, but also the grain structure and the lattice orientation in the grains, particle and phase distributions and the stresses and strains associated with the defects.

Calorimetric Studies of Recrystallization.

N. Hessel Andersen and D. Juul Jensen, In: Microstructural Characterization of Materials by Non-Microscopical Techniques. Proceedings of the 5th Risø International Symposium on Metallurgy and Materials Science, Risø, 3-7 September 1984. Edited by N. Hessel Andersen et al. (Risø National Laboratory, Roskilde, 1984) 181-186.

Microcalorimetric measurements have been used to study the recrystallization process of two materials, pure Cu (99.98%) and commercially pure Al (99.4%), deformed by cold-rolling to 95% and 90% reduction in thickness, respectively. The stored energy of cold work of Cu and Al has been measured by scanning calorimetry using a constant heating rate. The time dependence of the isothermal heat release of Cu has been determined at 6 temperatures from 420 K to 470 K.

Måling af Tykkelsen af Tynde Belægninger ved Energidispersiv Røntgenanalyse (Measurement of the Thickness of Thin Layers by Energy-Dispersive X-ray Analysis).

J.B. Bilde-Sørensen, In: Overfladebehandling - Processer og Egenskaber (Surface Treatment - Processes and Properties). Dansk Metallurgisk Selskabs Vintermøde, Skjoldenæs-holm, 4-6 Januar 1984. Edited by E.W. Langer and G. Skjels-ager (Dansk Metallurgisk Selskab, Lyngby, 1984) 173-183.

Energy-dispersive X-ray analysis is primarily used for elemental analysis but can also be used to measure the thickness of thin homogeneous layers on homogeneous substrates. Various methods relying on calibration standards are discussed. The method by Bishop and Poole based on pure standards only is described.

A Model for Deformation-Enhanced Recovery During and after Creep.

J. B. Bilde-Sørensen, In: Proceedings of the Second International Conference on Creep and Fracture of Engineering Materials and Structures, University College, Swansea, 1-6 April 1984. Edited by B. Wilshire and D.R.J. Owen (Pineridge Press, Swansea, 1984) 39-50.

The various versions of the dislocation network recovery model for creep have described the recovery of the network by the Friedel model or similar models which predict that the change in average link length per time unit is inversely proportional to the average link length. However, experimental results from the literature on the annealing of creep-induced dislocation networks after a stress removal strongly indicate that the recovery process is enhanced by glide and thus depends on the strain history. A dislocation model is suggested in which sites for strong recovery are created by the glide process: the intersection of two dislocations of opposite sign creates strongly curved links which will contract under the influence of their line

tension and thereby lower the stress needed to break adjacent junctions. As the curved links contract, the recovery potential is lowered. The recovery rate therefore depends not only on the dislocation density but also on the strain history. The model considers the recovery rate under quasi-steady-state conditions as well as the annealing of the network after a stress removal. The model agrees well with experimental annealing curves from the literature. The implications for creep models are discussed.

Acoustic Emission during Deformation and Fracture Processes in Metals.

C.P. Debel, In: Microstructural Characterization of Materials by Non-Microscopical Techniques. Proceedings of the 5th Risø International Symposium on Metallurgy and Materials Science, Risø, 3-7 September 1984. Edited by N. Hessel Andersen et al. (Risø National Laboratory, Roskilde, 1984) 19-33.

The processes involved in the generation and propagation of acoustic emission stress waves, and their subsequent transformation into electrical signals are extremely complex. Consequently, the understanding of these processes remains limited, despite intensive studies, and most research carried out to date is of a qualitative nature only. This review considers the general characteristics of acoustic emission signals and the parameters most often used in their description. Moreover, acoustic emission related to deformation and fracture processes in metals are presented, and the sources responsible identified to the degree these are commonly recognised.

A Quantitative Comparison between the Texture and the Micro-Structure developing during Recrystallization.

N. Hansen, D. Juul Jensen and F.J. Humphreys, In: Microstructural Characterization of Materials by Non-Microscopical Techniques. Proceedings of the 5th Risø International Symposium on Metallurgy and Materials Science, Risø, 3-7 September 1984. Edited by N. Hessel Andersen et al. (Risø National Laboratory, Roskilde, 1984) 267-272.

The recrystallization kinetics of commercially pure aluminium (99.4%) have been investigated by neutron diffraction texture measurements, selected area channelling patterns, light microscopy and hardness measurements. The fraction recrystallized and the time for 50% recrystallization as determined by each method have been compared, and the applicability, accuracy and speed of the four techniques are discussed.

Recrystallization in Commercially Pure Aluminum.

B. Bay and N. Hansen, Met. Trans. 15A (1984), 287-297.

Recrystallization behavior in commercial aluminium with a purity of 99.4% was studied by techniques such as high-voltage electron microscopy, 100 kV transmission electron microscopy, and light microscopy. Sample parameters were the initial grain size (290 and 24 microns) and the degree of deformation (5 to 30 pct reduction in thickness by cold-rolling). It was found that the original grain boundary region is the preferred site for nucleation. A few intragranular nuclei were, however, also observed. The effectiveness of the nucleation sites is enhanced by the presence of intermetallic particles (FeAl_3), which start to become operative when the degree of deformation is raised from 15 to 30 pct. The temperature of nucleation and of recrystallization decreases when the degree of deformation is increased and the initial grain size is decreased. The recrystallized grain size follows the same trend and it is observed that the refinement of the recrystallized grain size caused by an increasing degree of deformation and decreasing initial grain size is enhanced by the FeAl_3 particles (when the degree of deformation is raised from 15 to 30 pct). Finally, the structural and kinetic observations are discussed and compared with results from an earlier study covering the recrystallization behaviour of commercial aluminium of the same purity deformed at higher degrees of deformation (50 to 90 pct. reduction in thickness by cold-rolling).

High-Temperature Strength of Oxide Dispersion-Strengthened Aluminium.

A.H. Clauer and N. Hansen, Acta Met. 32 (1984) 269-278.

The tensile flow stress of coarse-grained dispersion-strengthened Al- Al_2O_3 materials were measured as a function of temperature (77-873 K) and volume fraction (0.19-0.92 vol) of aluminium oxide. For the same material, the creep strength was determined as a function of temperature in the range 573-873 K. The modulus-corrected yield stress (0.01 offset) is found to be temperature independent at low temperature (195-472 K). Between 473 and 573 K, the yield stress starts to decrease with increasing temperature. At high temperatures (573-873 K), the modulus-corrected yield stress is approximately constant (except for the material with the lowest oxide content). The high-temperature values of the modulus-corrected yield stresses are approximately two-thirds of the low temperature value. During high-temperature creep, there is a definite indication of a threshold stress. This threshold stress is proportional to the Orowan stress and it does not fall below about 0.5-0.7 of the Orowan stress. During creep even at stresses near the threshold stress a dislocation structure develops consisting of dense tangles surrounding the larger particles and the particle clusters in addition to a coarse dislocation network. These structures may modify both the threshold stress and the matrix creep properties.

The Pinning by Particles of Low and High Angle Grain Boundaries during Grain Growth.

C.J. Tweed, B. Ralph and N. Hansen, Acta Met. 32 (1984) 1407-1414.

A study has been made using transmission electron microscopy of the pinning of grain boundaries in aluminium during grain growth by fine dispersions of alumina particles. The boundary parameters have been determined with precision and the pinning effects measured using an approach due to Ashby and coworkers. These estimates of local driving pressures have shown that they are similar for both the low- and the high-angle boundaries encountered in the samples. The pinning effects by particles at high-angle boundaries are in general accord with the model due to Zener whilst those at low angle boundaries are much higher than predicted by Zener. An explanation is offered.

The Development of Recrystallization Textures in Aluminium containing large Intermetallic Particles followed by Neutron and Electron Diffraction Measurements.

D. Juul Jensen, N. Hansen and F.J. Humphreys, In: Proceedings of the 7th International Conference on Textures of Materials. Noordwijkerhout, 17-21 September 1984. Edited by C.M. Brakman, P. Jongenburger and E.J. Mittemeijer (Netherlands Society for Materials Science, Zwijndrecht, 1984) 251-256.

The formation and growth of recrystallization nuclei in commercial purity aluminium (99.4%) containing large intermetallic particles has been followed by texture measurements using neutron diffraction, selected area channelling patterns and various microscopical techniques. It was found that there was prolific nucleation at the particles of grains having a wide spread of orientation. But, because these grains grew slowly, the randomisation effect of the particles did not dominate the final recrystallization texture.

On-Line Registration of ODF Changes during Recrystallization.

D. Juul Jensen, N. Hansen, J.K. Kjems and T. Leffers, In: Proceedings of the 7th International Conference on Textures of Materials, Noordwijkerhout, 17-21 September 1984. Edited by C.M. Brakman, P. Jongenburger and E.J. Mittemeijer (Netherlands Society for Materials Science, Zwijndrecht, 1984) 777-782.

Fast in-situ determination of several different $[hkl]$ pole figures during recrystallization enables on-line registration of the changes in the ODF during the process. In the present paper the experimental set-up is described, and the potential of the apparatus is demonstrated by a kinetic investigation of the recrystallization of two different materials, aluminium of commercial purity and pure copper, both cold-rolled to 95% reduction in thickness.

In-Situ Texture Measurements by Neutron Diffraction used in a Study of Recrystallization Kinetics.

D. Juul Jensen, N. Hansen, J.K. Kjems and T. Leffers, In: Microstructural Characterization of Materials by Non-Microscopical Techniques. Proceedings of the 5th Risø International Symposium on Metallurgy and Materials Science, Risø, 3-7 September 1984. Edited by N. Hessel Andersen et al. (Risø National Laboratory, Roskilde, 1984) 325-332.

A technique for a fast in-situ texture determination by neutron diffraction is described. By an on-line recording of texture changes, information about metallurgical processes can be obtained if such processes are accompanied by a change in texture. This is illustrated by a kinetic investigation of recrystallization of commercially pure aluminium.

Texture Development during Grain Growth in Pure Copper.

E. Grant, D. Juul Jensen, B. Ralph and N. Hansen, In: Proceedings of the 7th International Conference on Textures of Materials, Noordwijkerhout, 17-21 September 1984. Edited by C.M. Brakman, P. Jongenburger and E.J. Mittemeijer (Netherlands Society for Materials Science, Zwijndrecht, 1984) 239-244.

It is well known that the texture of cold drawn and recrystallised copper rods changes during grain growth at elevated temperatures. The $\langle 111 \rangle$ fibre component is observed to strengthen at the expense of the $\langle 100 \rangle$ component. Using a neutron diffraction method for fast, "in situ" pole figure measurement at the DR3 reactor at Risø, the kinetics of this texture change have been studied. The material used was 99.99% copper, and grain growth was performed isothermally at several different temperatures in the range 700-1100 K. A parallel investigation to characterise the change in specimen microstructure has been carried out. The initial and final grain size distributions have been studied with the aid of an automatic image analyser. The change in texture is seen to be a result of anomalous grain growth.

Small-Angle Neutron Scattering Study of γ' -Precipitation in NiAlTi.

W. Hein, W. Wagner, H. Wollenberger and D. Juul Jensen,
In: Microstructural Characterization of Materials by Non-Microscopical Techniques. Proceedings of the 5th International Symposium on Metallurgy and Materials Science, Risø, 3-7 September 1984. Edited by N. Hessel Andersen et al. (Risø National Laboratory, Roskilde, 1984) 279-284.

The decomposition of the ternary alloy Ni-5.0 at% Al-5.8 at% Ti was investigated by Small-Angle Neutron Scattering after thermal annealing in the temperature range between 773 K and 873 K. The influence of multiple scattering from magnetic domains in the ferromagnetic matrix was analyzed by varying the measurement temperature. From the scattering of the γ' -precipitates, the particle size and average interparticle distance is determined. The coarsening kinetics of the γ' -precipitates is outlined and discussed.

Fuel Performance Experiments in Scandinavia.

A. Hanevik, P. Knudsen and H. Mogard, Nuclear Europe, 4
No. 2 (1984) 12-15.

An overview is given of fuel performance investigations at Risø, Halden and Studsvik. The work at Risø includes a national program in which burnups exceeding 65,000 MWD/tU have been achieved. Two internationally sponsored projects provide well-characterized data set on fission gas release in high-burnup water reactor fuel that is subjected to power transients. Highly instrumented fuel tests are carried out in the OECD Halden reactor. These studies address two aspects of fuel performance: 1) fuel defect processes caused by mechanical and chemical interaction between the fuel and the cladding (PCI); 2) fuel response under conditions of adverse transients/severe accident sequences. At Studsvik a series of internationally sponsored fuel irradiation research projects have been or are being conducted. The main research topic is the PCI failure occurrence in LWR fuel at burnups in the range 10,000-40,000 MWD/tU.

The Risø Fission Gas Project - An Overview.

P. Knudsen, Res Mechanica 12 (1984) 313-320.

The Risø Fission Gas Project has provided experimental data on fission gas release from high-burnup water reactor fuel. The data are well-characterized with respect to pre-irradiation measurement, irradiation and post-irradiation examination, thus enabling their use in fuel performance code validation. The experimental data were obtained with 12 Zircaloy-clad UO₂ pellet fuel

pins, irradiated in a test assembly to an average of $32,000 \text{ MWD}(\text{tU})^{-1}$. Most of the fuel pins were submitted to short-term re-irradiation at increased power levels ("bump testing") in a test reactor in order to simulate postulated power increases late in life. The bump tests covered a range of bump terminal levels of $320\text{--}462 \text{ W cm}^{-1}$ (peak pellet), mostly with a hold time of 24 h. Extensive hot-cell examinations were performed of base-irradiated and bump-tested fuel pins. The fission gas release resulting from the bump testing was in the range 0-16%, increasing with peak pellet levels above 400 W cm^{-1} . Local fission gas releases were determined from retained-gas measurements on pellet size samples. Release of the fission product cesium as a function of local bump terminal level resembled the local fission gas release. The gas release measurements were corroborated by extensive ceramicographic examinations and pore size analysis.

Overview of Workshop on "Evaluation of Simulation Techniques for Radiation Damage in the Bulk of Fusion First Wall Materials".

T. Leffers, B.N. Singh, W.V. Green and M. Victoria,
Radiat. Eff. 83 (1984) 1-9.

The main points and the main conclusions of a workshop held June 27-30 1983 at Interlaken, Switzerland, are reported. There was general agreement among the participants that ideal simulation, providing unambiguous information about the behaviour of the first wall material, is at present out of reach. In this situation the route to follow is to use the existing simulation facilities in a concerted effort to understand the damage-accumulation processes and thereby create the background for prediction or appropriate simulation of the behaviour of the first wall material.

Diffusion af Kobber ind i Sølv ved lav Temperatur (Diffusion of Copper into Silver at Low Temperature).

T. Leffers, In: Overfladebehandling - Processer og Egenskaber (Surface Treatment - Processes and Properties). Dansk Metallurgisk Selskabs Vintermøde, Skjoldenæsholm, 4-6 January 1984. Edited by E.W. Langer and G. Skjelsager (Dansk Metallurgisk Selskab, Lyngby, 1984) 185-192.

A theoretical estimate is made of the diffusion of copper into silver in copper-silver composite lamellae at temperatures in the range $200\text{--}250^\circ\text{C}$. It is found that grain-boundary diffusion and pipe diffusion would make copper atoms penetrate about $25 \mu\text{m}$ into the silver in 70 years at 250°C . The contribution from bulk diffusion is insignificant.

Correlation between Texture and Line Width in F.C.C. Material with Deformation Twin Lamellae.

T. Leffers and D. Juul Jensen, In: Proceedings of the 7th International Conference on Textures of Materials, Noordwijkerhout, 17-21 September 1984. Edited by C.M. Brakman, P. Jongenburger and E.J. Mittemeijer (Netherlands Society for Materials Science, Zwijndrecht, 1984) 805-810.

The line width of the $\{111\}$ reflection is measured by neutron diffraction for different positions in pole figures of rolled single crystals and polycrystals of brass. In accordance with theory it is found that the lines are narrow when the reflecting planes are parallel to the lamellae of deformation twins in the specimen and wide when the reflecting planes are tilted relative to the twin lamellae. The observations point at the possibility of making off-Bragg pole figures for mapping of twin orientations (and orientations of other defects). The observations also demonstrate the special deformation behaviour of the matrix/twin composite.

Komposit (1): Ønskematerialer: lette, stive, stærke.

(Composite (1): Ideal Materials: light, stiff, strong).

H. Lilholt, Ingeniøren 10, 25 (1984) 18.

A brief description was given of fibre-reinforced materials, with details on mechanical and physical properties, as well as activities on an international and national level.

Fiberforstærkede Kompositmaterialer (Fibre Reinforced Composite Materials).

H. Lilholt, Risø-M-2462 (1984) 12 pp.

The fundamentals of the calculations of stiffness and strength of fibre-reinforced composite materials, in the shape of laminates, are presented. Test methods for measurement of the compressive strength of fibre reinforced composite materials are reviewed. Experiments are performed to establish the usefulness of two test methods. The basic equations for the stiffness and deformation of sandwich-elements are presented. Experiments are carried out to test the theoretical equations and the involved approximation.

**Egenskaber af Glasfiber/Polyester anvendt til 30 m Vingebjælke
(Properties of Glassfibre/Polyester used in a 30 m Wingspar).**

H. Lilholt and P. Brøndsted, Risø-M-2464 (1984) 22 pp.

The glass-polyester material used in a wingspar made by tape-winding was characterised. The density, fibre content, porosity and fibre orientation was measured. The mechanical properties in static tensile loading were measured. Supporting laminate calculations were performed to evaluate the experimental results.

**Utilization of the Isotopic Composition of Xe and Kr in Fission
Gas Release Research.**

M. Mørgensen, Risø-M-2437 (1984) 19 pp.

Two examples of how the measured fission gas isotopic composition can be used in the study of fission gas release phenomena are given. In the first example the ratios of Kr85/Kr86 in released and retained gas are used for calculation of the "average time" when the gas was released. This "average time" may be used in code qualification. In the second example the degree of conversion of unstable Xe135 to stable Xe136 is derived from the measured ratio of Xe136 to Xe131+Xe132. This conversion is of importance in the calculation of the total Xe generation during irradiation.

On the Hydrogenation Mechanism in Magnesium I.

A.S. Pedersen, J. Kjøller, B. Larsen and B. Vigeholm, In: Hydrogen Energy Progress V. Proceedings of the 5th World Hydrogen Energy Conference, Toronto, Canada, 15-20 July 1984. Edited by T.N. Veziroglu and J.B. Taylor (Pergamon Press, New York, 1984) 1269-1277.

The first time hydriding of spherical magnesium particles covered by a thin oxide layer and sieve-fractionated into narrow size distributions within the range 40-90 μm was followed by microgravimetry. The size distributions of the fractions were determined by semiautomatic image analysis. The hydridings were run at 402°C and 3 MPa hydrogen pressure after heating in helium. A dependence of the rate of hydridation on the heat treatment prior to reaction was observed and it is proposed that the heat treatment causes oxygen atoms to diffuse into the bulk metal and thereby break up the protective oxide layer. Based on the observed hydride propagation in the metal particles a statistical model for the hydriding of a particle is applied to the hydridation curves for a series of samples. The data are found to be in fine agreement with the proposed model. It is concluded that care must be taken when generalizing results from the hydridation of magnesium powders.

Long-Term Cycling of the Magnesium Hydrogen System.

A.S. Pedersen, J. Kjøller, B. Larsen, B. Vigeholm and J.A. Jensen. Int. J. Hydrogen Energy 9 (1984) 799-802.

Magnesium powder with a grain size of approximately 50 μm was hydrogenated for 30 min and dehydrogenated the same time at 390°C, 515 times. A moderate loss in hydrogen storage capacity was observed and was ascribed to a measured decrease in reaction kinetics as the cycle number increased. The time for maximum hydrogen absorption was found to depend significantly on cycle number while the time for maximum desorption was found to be virtually independent of cycle number.

Relative Role of Gas Generation and Displacement Rates in Cavity Nucleation and Growth.

B.N. Singh and A.J.E. Foreman, J. Nucl. Mater. 122 & 123 (1984) 537-541.

The abstract appeared in the previous progress report p. 69.

Cavity Formation in Aluminium Irradiated with a Pulsating Beam of 225 MeV Electrons.

B.N. Singh, J.B. Bilde-Sørensen, T. Leffers, L.S. Oznigov and V.V. Gann, J. Nucl. Mater. 122 & 123 (1984) 542-546.

The abstract appeared in the previous progress report p. 68.

Nucleation of Helium Bubbles on Dislocations, Dislocation Networks and Dislocations in Grain Boundaries during 600 MeV Proton Irradiation of Aluminium.

B.N. Singh, T. Leffers, W.V. Green and M. Victoria, J. Nucl. Mater. 125 (1984) 287-297.

High-purity aluminium (99.9999%) was irradiated with 600 MeV protons with a damage rate of 3.5×10^{-6} dpa/s. Irradiation with 600 MeV protons produces helium and hydrogen at the rate of 140 and 615 appm per dpa, respectively. Specimens irradiated at temperatures in the range 116 to 318°C to doses in the range 0.04 to 5 dpa were examined in a transmission electron microscope (TEM). The TEM investigation has shown that helium bubbles are formed on dislocations in the grains as well as dislocations in the grain boundaries. Dislocation nodal points whether present in dislocation walls or in grain

boundaries are found to be the most favourable sites for bubble nucleation. The mean diameter of the bubbles on individual dislocation lines are found to be larger than those for the bubbles in the matrix. The bubble size and density on grain boundaries vary from boundary to boundary. The size of these bubbles on the boundaries is larger than or equal to the size of those in the matrix. It is suggested that helium atoms once arrived at a dislocation remain bound to the dislocation line but at the same time remain mobile within the dislocation core; the bubble nucleation behaviour in the core would thus be affected by the core structure of the different dislocations. An estimate of the effective helium diffusion in the dislocations relative to that in the lattice has been made on the basis of the measured bubble parameters and the width of the bubble-denuded zone along dislocation lines; the diffusion coefficient of helium in the dislocations is found to be about the same as that in the lattice.

Grain Boundary Related Effects in Aluminium during 600 MeV Proton Irradiation at Different Temperatures.

B.N. Singh, T. Leffers, W.V. Green and M. Victoria, J. Nucl. Mater. 122 & 123 (1984) 703-708.

The abstract appeared in the previous progress report p. 68.

Helium Bubbles in 600 MeV Proton-Irradiated Aluminium Studied by Positron Annihilation Technique.

K.O. Jensen, B.N. Singh, M. Eldrup, M. Victoria and W.V. Green, In: Microstructural Characterization of Materials by Non-Microscopical Techniques. Proceedings of the 5th Risø International Symposium on Metallurgy and Materials Science, Risø, 3-7 September 1984. Edited by N. Hessel Andersen et al. (Risø National Laboratory, Roskilde, 1984) 333-340.

Aluminium samples containing He-bubbles produced by 600 MeV proton irradiation at 120, 140, and 430°C were investigated by Positron Annihilation Technique (PAT); both lifetime and angular correlation measurements were made. In the low-temperature irradiated samples, changes in the lifetime of trapped positrons with dose and temperature are correlated with the bubble size. From the lifetime the He-density in the bubbles is estimated to be $7 \pm 4 \times 10^{22} \text{ cm}^{-3}$. The 430°C irradiated samples exhibit an unusually narrow angular correlation curve component associated with positronium formation in the bubbles, probably a result of transmutation produced Na segregating at the bubble surfaces.

Characterization of Helium Bubbles in High-Purity Aluminium by Small-Angle Neutron and X-ray Scattering.

J.K. Kjems, B.N. Singh, B. Sjöberg, M. Victoria and S.L. Green, In: Microstructural Characterization by Non-Microscopical Techniques. Proceedings of the 5th International Symposium on Metallurgy and Materials Science, Risø, 3-7 September 1984. Edited by N. Hessel Andersen (Risø National Laboratory, Roskilde, 1984) 355-362.

High-purity aluminium (99.999%) was irradiated with 600 MeV protons at the Swiss Institute for Nuclear Research (SIN), Switzerland. Subsequently, the specimen was studied with small-angle neutron and X-ray scattering techniques (SANS and SAXS). The bubble parameters determined by these techniques are compared with parameters obtained by transmission electron microscopy (TEM) on the same specimen. The size distribution of helium bubbles obtained from scattering measurements and TEM are found to be in good agreement. However, a noticeable difference in the X-ray and neutron scattering was observed; the difference could not be directly related to the helium content in the bubbles. Instead, the difference may be related to other impurities such as Mg provided they segregate near the bubble surface.

The Temperature Dependence of Void and Bubble Formation and Growth in Aluminium During 600 MeV Proton Irradiation.

M. Victoria, W.V. Green, B.N. Singh and T. Løffers.
J. Nucl. Mater. 122 & 123 (1984) 737-742.

The abstract appeared in the previous progress report p. 68.

Joint Nordic-German Symposium on Thermal Analysis and Calorimetry, Copenhagen, 24-26 August 1983.

P.J. Møller, O.T. Sørensen and A. Kettrup (editors).
Proceedings of the Joint Nordic-German Symposium on Thermal Analysis and Calorimetry, Thermochim. Acta 72 (1984) 1-262.

Symposium proceedings - 36 contributed papers in Thermal Analysis and Calorimetry.

Magnesium as an Energy Material.

B. Vigeholm, In: Proceedings of the 41st World Magnesium Conference, London 10-13 June 1984. (International Magnesium Association, Dayton, Ohio, 1984) 59-63.

Magnesium reacts reversibly with hydrogen to form magnesium hydride which is one of the most dense artificial energy storages. With hydrogen as a non-polluting energy vector, the storage system has a potential beyond the present economical competitiveness. A status is given of recent research into the Mg-H₂ system with emphasis on the properties relevant to practical use. Implemented and suggested applications are discussed.

On the Hydrogenation Mechanism in Magnesium II.

B. Vigeholm, J. Kjøller, B. Larsen and A.S. Pedersen, In: Hydrogen Energy Progress V. Proceedings of the 5th World Hydrogen Energy Conference, Toronto, Canada, 15-20 July 1984. Edited by T.N. Veziroglu and J.B. Taylor (Pergamon Press, New York, 1984) 1455-1463.

A metallographic study of the initial hydride formation in magnesium particles, < 100 µm diameter and thinly coated by 15-20 nm oxide was made. After a heat treatment in pure helium at 400°C for one hour and a subsequent exposure to 3 MPa hydrogen at 400°C we found the formation of surface nuclei to be the rate determining process. Following the hydrogen reaction from $\alpha = 0.1$ to $\alpha = 1$ we concluded that the transformation of a single particle - starting with one (rarely two) nucleus - was completed in a small fraction of the time needed to transform the entire sample. The extreme sensitivity of the transformation mechanisms to changes in surface oxide, particle morphology, manufacturing process and repeated reactions is demonstrated and discussed.

Effect of Oxygen on the Magnesium - Hydrogen Reaction.

B. Vigeholm, J. Kjøller, B. Larsen and A.S. Pedersen, J. Less Common Metals, 104 (1984) 141-148.

Two identical samples of magnesium powder (99.58% Mg) were hydrogenated at approximately 30 bar, 380°C and dehydrogenated under vacuum at the same temperature nearly 500 times. The first sample was exposed to 99.9999% pure hydrogen, the second to hydrogen containing 85 ppm oxygen and 8 ppm water vapour. In both experiments a moderate, overall reduction in adsorbed/desorbed amount of hydrogen was observed. This may be ascribed to reduced absorption rate with increased number of cycling. The effect of oxygen was negligible,

which was confirmed by precision absorption measurement after the cycling experiment. Despite the decreased absorption rate - mainly at higher degrees of reaction little change in desorption kinetics was observed.

LECTURES

Determination of the Irradiation Time Elapsed After Release of Volatile Fission Gas Products in Water Reactor Fuel.

C. Bagger and M. Mogensen, presented at the IAEA Specialists' Meeting, Tokyo, 26-30 November 1984. (Transcript available).

Unintentional power excursions causing release of volatile fission products in water reactor fuel may occur during long term irradiation, e.g. by control rod movement. Two independent methods based on post-irradiation measurements are described for determination of the time of such releases. One method is based on measurement of the ratio between the ^{137}Cs radioactivity at the rim and at the center of a fuel cross section. The build-up of ^{137}Cs as a function of time is computed from the power history. Calculation of the time of a transient from the experimentally determined ^{137}Cs ratio is enabled by assuming a fractional ^{137}Cs release in the fuel center of known magnitude. In case of several transients the time of the last one is determined. The second method is based on measurement of the $^{85}\text{Kr}/^{86}\text{Kr}$ ratio in retained and in released fission gas. In the retained gas the ratio changes along the irradiation due to production and radioactive decay, while decay, only, is responsible for changes in the released gas. This enables calculation of the release time of the fission gas. In case of several transients the "average age" of the released gas is determined.

Moderne Udmattelsesprøvning - Udstyr og Metoder

(Modern Fatigue Testing - Equipment and Methods).

P. Brøndsted, presented at a conference on Mechanical Testing of Materials, Mariehamn, Finland, 23-25 October 1984. (Transcript available).

Servocontrolled test machines for fatigue testing are described. The construction and the control of the servohydraulic, the servoelectric, and the resonance machines are illustrated. Test methods for measuring time to failure, crack initiation, and crack growth based on statistical structural methods and fracture mechanics are illustrated by examples.

Fracture Mechanics Testing of Materials Toughness.

C.P. Debel, presented at a conference on Mechanical Testing of Materials, Mariehamn, Finland, 23-25 October 1984. (Transcript available).

A number of currently available as well as proposed standard test methods, based on the concepts of fracture mechanics, for testing of materials fracture toughness are presented. Difficulties and limitations are addressed.

Irradiation Embrittlement of Weldments in PV Steels.

C.P. Debel and F. Adrian, presented at an IAEA Specialists' Meeting, Vienna, 11 October 1984. (Available as Risø-I-150).

This third progress report on the IAEA-Programme: "Analysis of the Behaviour of Advanced Pressure Vessel Steels under Neutron Irradiation" presents the final analysis of fracture tests carried out on unirradiated control specimens at various temperatures within the operating envelope of a nuclear pressure vessel.

Fracture Toughness Evaluation of Pressure Vessel Steel by Small Three-Point-Bend Specimens.

S. Chatterjee and C. Debel, presented at the 6th International Conference on Fracture, New Delhi, 4-10 December 1984. (Proceedings to be published).

J_C fracture toughness tests by three point bending were conducted using several pre-cracked CNV specimens made from HAZ of pressure vessel steel materials. The test temperatures ranged from ambient temperature to 290°C, and the deformation speed was 0.25 mm/min. the test procedure adopted was based mainly on the multi-specimen standard practice for J_{IC} testing recommended by ASTM E813:81, even though it was recognised that the requirements of specimen size would hardly be met, especially for unirradiated materials. This paper discusses the results and suggests a suitable equation for the blunting line in the R-curve method and the procedure for determination of J_{IC} for irradiated specimens using such small specimens.

Polycrystalline Strengthening.

N. Hansen, presented at the TMS-AIME Fall Meeting, Detroit, 16-20 September 1984. (Proceedings to be published).

The strength of polycrystalline specimens can be related to interaction phenomena taking place during elastic and plastic deformation. Such phenomena are reviewed in terms of macroscopic and microscopic strain accommodation processes required to maintain strain continuity across the grain boundaries. The strength-grain size relationships can be described in a number of empirical equations relating the yield stress and the flow stress in tension to various structural parameters. A number of such equations are reviewed and their predictive capability is discussed.

Role of Dislocations, Dislocation Walls and Grain Boundaries in Void Formation During Early Stages of Fast Neutron Irradiation.

A. Horsewell and B.N. Singh, presented at the 12th International Symposium on the Effects of Radiation on Materials, Williamsburg, Virginia, USA, 18-20 June 1984. (Proceedings to be published).

High purity aluminium was used to study the details of microstructural evolution during early stages of neutron irradiation. Aluminium specimens were irradiated at 120°C to fluences between $2 \cdot 10^{21}$ and $1 \cdot 10^{24}$ n.m⁻² ($E > 0.1$ MeV). TEM investigation demonstrated that even in fully annealed material irradiation induced dislocations and voids evolve heterogeneously. In addition, voids and dislocations were found to segregate such that the groups of voids and dislocations are spatially separated from each other. This kind of heterogeneity and segregation is further enhanced by the introduction of microstructural heterogeneity (in the form of dislocation walls) prior to irradiation. Another form of heterogeneity was found to occur in a relatively wide band in the vicinity of the void denuded zone along grain boundaries; in this region, both formation and growth of voids were enhanced compared to that observed in the grain interior. It is argued that these results cannot be rationalized in terms of a conventional bias driven mechanism operating in a continuous sink medium. Both cell size and grain boundary effects would indicate an unusually high rate of transport of self-interstitial atoms from cell- and grain-interiors to cell walls and grain boundaries.

Thermal Expansion of Glass Fibre Reinforced Polyester.

H. Lilholt, presented at the Gordon Conference on Composites, Santa Barbara, California, 16-20 January 1984. (Not available).

Measurements of thermal expansion of pultruded materials of glass/polyester have been compared with calculated values of the thermal expansion.

Creep of Composite Materials.

H. Lilholt, presented at the Materials Research Laboratory, Pennsylvania State University, Pennsylvania, 23 January 1984, and at the Center for Composite Materials, University of Delaware, Delaware, 26 January 1984. (Not available).

A presentation was given of the models for creep of fibrous composite materials, with special reference to composites with metallic matrices.

Keramiske Fibre og Kompositmaterialer (Ceramic Fibres and Composite Materials).

H. Lilholt, presented to Dansk Støberiteknisk Forening, Risø, 18 February 1984. (Not available).

A presentation was given of fibres, their properties, and composite materials with metallic matrices. The fabrication methods were reviewed.

Strength Contributions during Creep of Composite Materials.

H. Lilholt, presented at the IUTAM Eshelby Memorial Symposium on Fundamentals of Deformation and Fracture, Sheffield, UK, 2-5 April 1984. (Proceedings to be published).

The characteristics of creep behaviour of composite materials with aligned fibres are reviewed. A model for composites with rigid fibres is presented, and strengthening factors are worked out. Based on the analysis of internal stresses and strains by J.D. Eshelby several contributions to the creep strength are evaluated. A model for the behaviour of composites with creeping fibres is included, and the transition from rigid-fibre behaviour to creeping-fibre behaviour is demonstrated. The advantage of combined analyses of several sets of data is emphasized and demonstrated for a set of experimental data. These analyses show the possibility of deriving equations for the (in situ) properties of the fibres. It is also shown that a friction stress could possibly exist in certain composites with coarse microstructure, the nature of the friction stress can not be established. The analogous situations in tensile, plastic deformation and in creep deformation are illustrated for materials both in the unrelaxed state and in the relaxed state.

Kompositmaterialer (Composite Materials).

H. Lilholt, presented at ATV's Møde om Plastmaterialer til Apparatkonstruktion, DTH, Lyngby, 9 April 1984. (Not available).

A review was given of fibres, their properties, their composites; the mechanical properties of fibrous composite materials were presented; the principles of fabrication were discussed.

Creep of Fibrous Composite Materials.

H. Lilholt, presented at the Conference on Composites, Materials and Engineering, University of Delaware, Delaware, 24-28 September 1984. (To appear in Composites Science and Technology).

Models for the creep behaviour of fibrous composite materials with aligned fibres are presented. The models comprise both cases where the fibres remain rigid in a creeping matrix and cases where the fibres are creeping in a creeping matrix. The treatment allows for several contributions to the creep strength of composites. The advantage of combined analyses of several data sets is emphasized and illustrated for some experimental data. The analyses show that it is possible to derive creep equations for the (in situ) properties of the fibres. The experiments treated include model systems like Ni + W-fibres, high temperature materials like Ni + Ni₃Al + Cr₃C₂-fibres, and medium temperature materials like Al + SiC-fibres. For the first two systems reasonable consistency is found for the models and the experiments, while for the third system too many unquantified parameters exist and further studies seem necessary.

Styrke og Deformationsforhold for Plastkompositter (Strength and Deformation Aspects of Resin Composites).

H. Lilholt, presented to Dansk Forening for Apparatteknik, DTH, Lyngby, 10 October 1984. (Not available).

A review of mechanical properties of composite materials was presented.

Kompositmaterialernes Udvikling og Anvendelse (The Development and Application of Composite Materials).

H. Lilholt, presented to Dansk Forening for Apparatteknik, DTH, Lyngby, 10 October 1984. (Not available).

A brief presentation was given of trends in the future developments for composite materials, with special reference to Danish industry.

Kompositmaterialernes Egenskaber (The Properties of the Composite Materials).

H. Lilholt, presented at Metallurgiafdelingens Industrimøde, Risø, 29 November 1984. (Not available).

A presentation was given of stiffness, strength, fatigue and creep properties of fibrous composite materials.

Materialeproblemer (Materials Problems).

H. Lilholt, presented at Risø's Dag om Vindenergi, Risø, 11 December 1984. (Not available).

Materials for wingblades for windturbines were discussed, especially glassfibre reinforced polyester. Properties like density, stiffness and strength were presented. Fatigue properties and possible design- and testing procedures for wingblades were discussed.

Fremstillingsteknologi for Fiberforstærket Plast (Fabrication Technology for Fibre Reinforced Plastics).

Aa. Lystrup, presented at Metallurgiafdelingens Industrimøde, Risø, 29 November 1984. (Not available).

Filament winding and autoclave curing of pre-preg laminates are some of the manufacturing processes for fibre reinforced plastics. The technology and the equipment at the Metallurgy Department are described, with emphasis on the most important process parameters. As examples of applications a filament wound pressure vessel and an autoclave cured kayak paddle are shown.

Analysis of the RFGP Experiments by the Fuel Performance Codes FRP and URANUS.

I. Misfeldt and K. Lassmann, presented at the IAEA Specialists' Meeting on Water Reactor Fuel Element Performance Computer Modelling, Bowness - on - Windermere, UK, 9 - 13 April 1984. (Proceedings to be published).

The Risø Fission Gas Project (RFGP) experiments have been analysed by the integral fuel performance codes FRP and URANUS. The paper presents the results from both codes used with their standard models for gas release. The calculations have demonstrated that there is good agreement between the codes with regard to the calculated fuel temperatures; any deviations could be explained in terms of differences in the models for gas release, swelling and densification. Both models included the NRC burnup enhancement factor and thereby reached reasonable agreement with the experimental results. The analysis included calculations with a number of simple gas release models, e.g. temperature-zone models and those based on diffusion. Common for the models based on diffusion was a significant underprediction of the release during the short EOL bump tests. Temperature-zone models without burnup enhancement also underpredicted the release significantly.

Lithium Batterier med Flydende Katode (Lithium Batteries with Liquid Cathode).

M. Mogensen, presented to Dansk Elektrokemisk Forening, Søborg, 30 May 1984. (Not available).

The compounds which are used as liquid cathodes in lithium batteries were described. The effective electrolytes in such cells are spontaneously formed thin solid passivating layers which are Li^+ conductors. The advantages of the two most important commercial systems (Li/SO_2 and Li/SOCl_2) are the extremely high power and energy densities. A comparison between these and older types such as lead/acid and Zn/MnO_2 was given. There are three major disadvantages of the Li-liquid cathode batteries: 1) They are not rechargeable, 2) they cause safety problems, and 3) they show delayed voltage when used after long time storage. The delayed voltage problem (or time dependent passivation problem) was treated in details. Measurement techniques were described together with results obtained at Risø. The "state of the art" with respect to the understanding of the passivation mechanisms was presented.

The A.C. Response of Lithium, Stainless Steel, and Porous Carbon Electrodes in Thionyl Chloride solutions.

M. Mogensen, presented at The 2nd International Meeting on Lithium Batteries, Paris, 25-27 April 1984. (To appear in J. Power Sources).

Impedance measurements on Li electrodes in SOCl_2 electrolytes indicate that the structure of the passivating surface layer formed in 1.8M LiAlCl_4 differs from that formed in 1.8M AlCl_3 , 1.2M LiCl , 0.6M SO_2 . Also, porous carbon electrodes are found to behave differently in these two electrolytes. Unpolarised stainless steel electrodes show a 67° constant phase angle impedance over a wide frequency range whereas polarised to 0 mV vs. Li the

impedance diagram is very similar to that of Li. Finally, it is found that passivation may develop differently for Li pressed onto stainless steel from that of Li pressed onto glass.

Mean Field Theory and the Bauschinger Effect in Composites.

O.B. Pedersen, presented at the IUTAM Eshelby Memorial Symposium on Fundamentals of Deformation and Fracture, Sheffield, UK, 2-5 April 1984. (Proceedings to be published).

The development of a rigorous mean field theory for dense thermoelastic composites from J.D. Eshelby's independent inclusion approximation for dilute elastic composites is outlined. The concept of an effectively uniform plastic strain in the matrix enables the mean field theory to give an accurate quantitative account of mean phase stresses measured by X-ray diffraction in metallic fibre composites. The mean in-situ friction stress in the matrix can be understood as an addition of plastic friction due to misfits equivalent with Orowan loops and elastic friction due to misfits arising from elastic heterogeneity. An analysis suggests that the plastic friction may be measured separately in a Bauschinger experiment if elastic friction adds linearly to plastic friction.

Hardening Mechanisms in Metallic Composites.

O.B. Pedersen, presented at the Institute of Material's Science, Tampere University of Technology, Tampere, Finland 3 May 1984. (Not available).

The low temperature strength of metal matrix composites was discussed in terms of a continuum model and dislocation mechanisms. Observations of the evolution of the dislocation microstructure in the unreinforced matrix were summarized in hardening diagrams.

Plasticity of Single Crystals and Polycrystals - Hardening Diagrams.

O.B. Pedersen, presented at the Euromech 183 Colloquium on Plasticity of Crystalline Media, Villetaneuse, France, 24-27 September 1984. (Not available).

Recent experimental and theoretical work show that the linear theory of composites can be combined with the dislocation theory of obstacle controlled flow to give a unified view of the micromechanisms of strain hardening in crystalline matter. A summary of this view will be given by using the idea of "hardening diagrams", in which the plastic strain amplitude is taken as

one axis and the cycle number as the other axis. Observed boundaries between different regimes of hardening, and between transitions from one stage of hardening to the next, are drawn in the diagrams. In this way the fields governed by each hardening mechanism are displayed. The hardening diagrams are constructed mainly from measurements of monotonic hardening rates and of the sizes and shapes of stress-strain loops in cyclic hardening at constant plastic strain amplitudes. Observations of the hardening behaviour by different experiments are fairly consistent, and they are closely correlated with microstructural observations obtained by a variety of microscopical and non-microscopical techniques. At present the most comprehensive data set is for copper single crystals deformed in single slip; but recent work allows a reasonably detailed hardening diagram to be constructed for copper polycrystals. The existing data for the other face-centred cubic metals suggest that their hardening diagrams will not differ qualitatively from those of copper. The existing data are also sufficient for giving a general outline of the influence of various parameters on the hardening diagrams: single crystal orientation, texture, grain-size, particles, solutes and temperature. The diagrams give an instructive overall picture for a given material of the successive processes of plastic flow at low temperatures; but they have several limitations: mainly they are limited to hardening associated with dislocation microstructures evolving along one particular type of strain path, paths of constant plastic strain amplitudes. The effect of the strain path will therefore be discussed in the light of recent theory and existing data. Furthermore, the diagrams do not include temperature and strain-rate effects. They are therefore complementary to Ashby's deformation-mechanism maps, which display the temperature and strain-rate effects in deformation without hardening.

Plasticity of Fibre Composites - In-Situ Hardening Mechanisms.
O.B. Pedersen, presented at the Euromech 183 Colloquium
on Plasticity of Crystalline Media, Villetaneuse. France,
24-27 September 1984. (Not available).

It is still unclear whether the linear theory of composites can be combined with the dislocation theory of obstacle controlled flow to explain the hardening behaviour of metal matrix fibre composites. In particular, there is a striking quantitative difference between the hardening mechanisms acting in the matrix of a fibre composite and those summarized in the hardening diagrams for unconstrained metals: in-situ measurements of mean phase stresses by X-ray diffraction shows matrix hardening rates in fibre composites as high as 0.5 times μ , the elastic shear modulus of the matrix. Comparable hardening rates for the unconstrained metal are less than about 0.003 times μ . The X-ray data show clearly that this "constraint effect" cannot be explained in terms of multiaxial matrix mean stresses. Recent work, however, shows that it is possible to combine a simple mean field theory, equivalent with the established linear theory of bounds for thermoelastic composites, with the concept of an effectively uniform plastic strain in the matrix. This approach seems to work when applied to the X-ray data. It shows very clearly

that the mean matrix stress consists of an "elastic" term and a "plastic" term, and that the plastic term is reduced by stress relaxation. When the approach is combined with the concepts of an effectively uniform in-situ friction stress in the matrix and a Tresca type yield criterion it suggests that the X-ray data can be understood in terms of a "plastic" friction stress and an "elastic" friction stress. Both friction stresses can be described in terms of the theory of obstacle controlled dislocation glide. In terms of continuum plasticity the plastic friction is isotropic; but the elastic friction adds a kinematical hardening contribution to the in-situ matrix hardening whenever the composite as a whole displays a Bauschinger effect. A simple model of the Bauschinger effect emerges from the directional properties of the elastic and plastic components of the matrix mean stress and the matrix friction stress. This model suggests the possibility of separating the plastic friction from the three other hardening components by measuring the composite's Bauschinger effect. Preliminary Bauschinger data for copper single crystals containing up to 40 vol. pct. tungsten fibres suggest that the plastic friction is proportional to the unrelaxed plastic strain in the matrix.

Solid-Electrolyte Research in Denmark.

F.W. Poulsen, presented to the Department of Metallurgy and Materials Science, Imperial College, London, UK, 19 January 1984. (Not available).

Batteries, fuel cells, and gas sensors with improved performance can be constructed using solid-electrolytes. The search for and characterisation of sodium, lithium, fluorine, and oxygen ion conductors carried out at 4 different institutions in Denmark are presented.

Materialer til Avancerede Batterier (Materials for Advanced Batteries).

F.W. Poulsen, presented to Dansk Forening for Materialografi, Kolding, 15-16 November 1984. (Not available).

Most materials used in advanced batteries are sensitive towards oxygen, water, and nitrogen. The special techniques for handling materials in glovebox systems and transferring them to analytical equipment are discussed. The lecture is accompanied by a demonstration of basic properties of Li-metal and solid electrolytes developed at Risø.

New Superionic Conductors of the Alkaline Metal - Hexachlorometallate Family.

F.W. Poulsen, N.H. Andersen and K. Clausen, presented at the EUCHEM Conference on Solid State Chemistry and Electrochemistry, St. Catherines College, Oxford, UK, 19-23 March 1984. (To appear in Solid State Ionics).

A whole range of superionic conductors appears to exist in the group of materials of the general formula $MM'Cl_6$, where M is an alkaline metal and M' is niobium or tantalum. Recent results from studies of conductivity, DSC and neutron diffraction are reported. In general, the compounds pass through one or two phase transitions above room temperature before reaching the conductive phase. For $KTaCl_6$ the conductivity at 300°C amounts to ~ 0.2 $(\text{ohm}\cdot\text{cm})^{-1}$.

Conductivity and Neutron Diffraction Studies of Solid Electrolyte-Melt Transitions.

F.W. Poulsen, N.H. Andersen and K. Clausen, presented at the EUCHEM Conference on Molten Salts, Elsinore, Denmark, 19-24 August 1984. (Not available).

Combined neutron diffraction and ionic conductivity studies have been used in characterising different types of melt processes. Congruent-, incongruent-, and sublattice melting have been observed in $TeCl_4$, $LiBiO_2$, and $KTaCl_6$ respectively.

Implications of High Energy Radiation Damage to Materials Performance.

B.N. Singh, presented at the Institut für Festkörperforschung, Kernforschungsanlage Jülich, 26 April 1984. (Not available).

Whilst considering materials for their use in an environment where they will be exposed to radiation with high energy particles, two major effects of radiation damage on materials behaviour must be evaluated: the effect of radiation damage on (a) dimensional stability and (b) mechanical properties. In the present talk, first of all, the origin of these effects will be described. This will be followed by identification of radiation and structural parameters controlling the magnitude of the damage effects. Finally, the ways and means of limiting the degree of detrimental damage (i.e. improving in-service lifetime) will be discussed.

Some Aspects of Defect Accumulation during Irradiation.

B.N. Singh, presented at the Institut de Génie Atomique, Ecole Polytechnique Fédérale de Lausanne, 23 July 1984. (Not available).

During irradiation at elevated temperatures lattice defects cluster and agglomerate. Factors controlling the clustering of defects will be described. The role of irradiation parameters and microstructural variables in defect accumulation will be discussed.

Evolution of Microstructure during Irradiation.

B.N. Singh, presented to the Materials Science Laboratory, Reactor Research Centre, Kalpakkam, India, 21 November 1984. (Not available).

Experimental results on microstructural evolution in high-purity aluminium irradiated with fast neutrons and high-energy (600 MeV) protons will be described. The influence of dislocations, dislocation walls and grain boundaries on void nucleation and growth will be described. The effect of sub-grain size on void swelling will be compared and contrasted with the effect of grain size on void swelling during HVEM irradiation.

Materials Response to Irradiation under Fusion Conditions.

B.N. Singh, presented to the Indian Physics Association, Reactor Research Centre, Kalpakkam, India, 23 November 1984. (Not available).

In the present talk the problem of plasma-wall interaction and the effects of 14 MeV neutron (produced as a result of fusion reaction) irradiation on dimensional stability and mechanical properties of the first wall material will be considered. Some experimental and theoretical results showing the effect of high helium generation rate will be described and discussed.

Irradiation Induced Defect Accumulation and its Consequences.

B.N. Singh, presented to the Department of Metal Science and Technology, Kyoto University, Kyoto, Japan, 10 December 1984. (Not available).

The accumulation of irradiation induced defects leads to void swelling in metals and alloys. Effects of alloying and cold-work on void nucleation and growth will be described and discussed.

Theoretical and Experimental Aspects of Cavity Nucleation during Irradiation.

B.N. Singh, presented at the Research Institute for Applied Mechanics, Kyushu University, Fukuoka, Japan, 12 December 1984. (Not available).

A physical (rather than a statistical) model for cavity nucleation will be presented. The problem of stability (configurational and spatial), diffusion and agglomeration of vacancy-gas atom complexes will be considered. Some of the numerical results of the model will be compared with experimental results.

Development of Microstructural Heterogeneity during Irradiation.

B.N. Singh, presented to the Department of Nuclear Engineering, University of Tokyo, Tokyo, Japan, 14 December 1984. (Not available).

During irradiation lattice defects (i.e. self-interstitials and vacancies) are generated homogeneously. TEM examinations of some neutron irradiated metals have shown, however, that the microstructural evolution occurs in a very heterogeneous fashion. Experimental evidence illustrating the development of microstructural heterogeneities will be presented. The problem of nucleation and growth of heterogeneities will be discussed.

Bubble Nucleation in Grain Interior and its Influence on Helium Accumulation at Grain Boundaries.

A.J.E. Foreman and B.N. Singh, presented at the First International Conference on Fusion Reactor Materials, Tokyo, Japan 3-6 December 1984. (To appear in J. Nucl. Mater.).

In the present paper we discuss the development of heterogeneous microstructure for uniform irradiation conditions. It is shown that microstructural inhomogeneities on a scale of 0.1 μm can develop purely from kinematic considerations because of the basic structure of the rate equations used to describe such evolution. Two aspects of the growth of such inhomogeneities are discussed. Firstly, it is shown that a local variation in the sink densities of the various microstructural defects will tend to enhance the inhomogeneity rather than remove it. Secondly, such inhomogeneities will lead to point defect fluxes that result in a spatial growth of the inhomogeneous region, which will be stopped only when the microstructural density around this region becomes large. The results have important implications in the formation of denuded zones and void formation in metals.

Inhomogeneous Microstructural Growth by Irradiation.

K. Krishan, B.N. Singh and T. Leffers, presented at The 1st International Conference on Fusion Reactor Materials, Tokyo, Japan, 3-6 December 1984. (To appear in J. Nucl. Mater.).

The production of helium and hydrogen is relatively fast in the structural materials used for fusion devices, so that at elevated temperatures helium can accumulate at grain boundaries and cause embrittlement. The density of microscopic cavities formed in the grains during irradiation, which moderates the gas flux to the boundaries, can vary considerably under high gas production conditions. Thus the mechanisms responsible for the nucleation of voids and gas bubbles become very relevant and must be discussed. A diffusion calculation is made of the flux of helium atoms to a grain boundary, taking account of the denuded zones. The calculated accumulation of helium is in good agreement with the measured gas content of grain boundaries in a bulk irradiated material. This demonstrates that an appreciable density of gas bubbles, as found in some materials, can protect the boundaries from excessive deposition of gas.

Computer Controlled Thermogravimetric Stepwise Isothermal Analysis.

O. Toft Sørensen, presented at the Third European Symposium on Thermal Analysis and Calorimetry, Interlaken, Switzerland, 10-15 September 1984. (To appear in Thermochim. Acta).

A microprocessor system developed for Thermogravimetric Stepwise Isothermal Analysis is described. This system is especially useful in kinetic studies and, as an example, the results obtained in a study of the decomposition of Ce-carbonate are discussed. From this study it is concluded that the controlling mechanism for the first part of this reaction is three dimensional nuclei growth, whereas the last part is phase boundary controlled.

Oxygen Ionledere: Materialer, Egenskaber og Anvendelser (Oxygen Ionconductors: Materials, Properties and Applications).

O. Toft Sørensen, presented at Norges Tekniske Højskole, Trondheim, Norway, 16 November 1984. (Not available).

Introductory lecture to oxygen conductors and their applications in oxygen sensors, fuel cells and high temperature electrolyzers. Furthermore the new composite ceramics based on partially stabilized zirconium oxides was briefly discussed.

Damage in Angle-Ply Laminates.

H.L. Toftegaard, presented at a Symposium on Damage in CFRP Laminates, University of Surrey, Surrey, UK, 25 October 1984. (Not available).

A project on investigation of damage in carbon fibre reinforced plastic laminates was discussed together with a series of tests for lamina properties in terms of stiffness and strength. The methods used for manufacture and quality assurance were briefly given.

Prøvning af Fiberkompositter: Kul/Epoxy (Testing of Fibre Composites: Carbon/Epoxy).

H.L. Toftegaard, presented to Dansk Forening for Materialografi, Kolding, 15 November 1984. (Not available).

Methods for manufacturing, quality assurance and determination of stiffness and strength of carbon fibre reinforced epoxy were given.

Kvalitetssikring og Skadeundersøgelser I (Quality Assurance and Damage Investigations I).

H.L. Toftegaard, presented at Metallurgiaafdelingens Industri-møde, Risø, 29 November 1984. (Not available).

Methods for quality assurance and damage investigation of fibre reinforced plastic were given. Quality assurance methods included determination of fibres fraction, fibre orientation and interlaminar shear strength. Damage investigation methods included scanning electron microscopy, X-rays combined with an opaque penetrant and finally edge replica.

Risø's program for Brintlagring og Brændselscelle Udviklingen (Risø's Program for Hydrogen Storage and the Development of Fuel Cells).

B. Vigeholm, presented to ATV's gruppe 1, Risø, 30 October 1984. (Not available).

A survey was given of the past and present programme on materials research and systems development within energy storage based on metal hydrides. An outline of the recently initiated programme aiming at combining hydride systems with fuel cells was added.

Effect of Oxygen on the Mg-H Reaction.

B. Vigeholm, J. Kjøller, B. Larsen and A.S. Pedersen, presented at the International Symposium on the Properties and Applications of Metal Hydrides IV, Eilat, Israel, 9-13 April 1984. (To appear in J. Less-Common Metals).

Two identical samples of magnesium powder (99.58% Mg) were hydrogenated at approximately 30 bar, 380°C and dehydrogenated under vacuum at the same temperature nearly 500 times. The first sample was exposed to 99.9999% pure hydrogen, the second to hydrogen containing 85 ppm oxygen and 8 ppm water vapour. In both experiments a moderate, overall reduction in absorbed/desorbed amount of hydrogen was observed. This may be ascribed to reduced absorption measurement after the cycling experiment. Despite the decreased absorption rate - mainly at higher degrees of reaction - little change in desorption kinetics was observed.

Industriaspekter for Fiberforstærkede Materialer (Industrial Aspects of Fibre Reinforced Materials).

G. Waage Petersen, presented at Metallurgiafdelingens Industridag, Risø, 29 November 1984. (Not available).

Advantages, properties and use of fibrous composite materials.

STAFF OF THE DEPARTMENT
(as at 31 December 1984)

Niels Hansen, Head of Department

Scientific Staff

Adolph, E.
Andersen, J.N. 2)
Andersen, Sv.I. 3)
Bagger, C.
Bentzen, Janet
Bilde-Sørensen, J.B.
Borring, J. 1)
Brøndsted, P.
Carlsen, Hans
Christensen, Jørgen
Debel, C.P.
Domanus, J. 1)
Gundtoft, H.E.
Horsewell, A.
Hougaard, H.
Jensen, Arne 1)
Jensen, Dorthe Juul
Johansen, Bjørn S.
Knudsen, Per
Leffers, T.
Lilholt, H.
Lystrup, Aa.
Misfeldt, I. 1)
Mogensen, Mogens
Pedersen, A. Schrøder
Pedersen, O. Bøcker
Poulsen, Finn W.
Rørbo, K.
Schmidt, J.O.
Singh, B.N.
Soliman, E.E. Salah 2)
Sørensen, O. Toft
Toft, P. 1)
Toftegaard, H. Langmaack
Vigeholm, B.

Technical Staff

Adrian, F.
Andersen, Axel B.
Andersen, Palle
Arensbach, F. Hvid
Aukdal, J.A.
Brøns, J.
Bülow-Christensen, C.J.
Christensen, C. Frees
Christensen, Sv.E.
Cooper, D.

Dreves, P.
Frederiksen, Henning
Friedrichsen, U.J.
Gravesen, Niels N. 1)
Hersbøll, B.
Jacobsen, M.
Jensen, Finn
Jensen, Knud
Jensen, Palle V.
Jespersen, John 1)
Klitholm, C.
Kjøller, J.
Larsen, Bent
Larsen, Jan
Larsen, Kjeld J.C.
Lindbo, J.
Mikkelsen, Claus
Nielsen, Ove
Nielsen, Palle
Nielsen, Torben
Nilsson, H.
Olesen, Preben B.
Olsen, Arne
Olsen, Benny F.
Olsen, Bent
Olsen, Henning
Olsen, Ole 1)
Olsson, J.
Paulsen, Henrik
Pedersen, Børge
Petersen, Jan H.A.
Petersen, Knud E.
Rasmussen, Allan E.
Riis, L.
Sandsted, K. 1)
Strauss, T.R.
Sørensen, Erling 1)
Vig, T. Lauersen
Aagesen, Sven

Office Staff

Arildsen, Nina 1)
Dreves, Elsa
Frederiksen, Anelise
Hejlund, Ingelise
Lauritsen, Grethe W.
Szötz, Anni
Sørensen, Eva

- 1) Employee from the Atlas Advanced Engineering Division
2) Post-graduate student from the Technical University of Denmark
3) On leave at absence from the Engineering Department, Risø

**Sales distributors:
G.E.C. Gad Strøget
Vimmelskaftet 32
DK-1161 Copenhagen K, Denmark**

**Available on exchange from:
Risø Library, Risø National Laboratory,
P.O.Box 49, DK-4000 Roskilde, Denmark**

**ISBN 87-550-1103-9
ISSN 0106-2840**